Article (refereed) - postprint

Garneau, Cyril; Sauvage, S.; Sánchez–Pérez, J.–M.; Lofts, S.; Brito, D.; Neves, R.; Probst, A. 2017. **Modelling trace metal transfer in large rivers under dynamic hydrology: a coupled hydrodynamic and chemical equilibrium model**.

Modelling trace metal transfer in large rivers under dynamic hydrology: a coupled hydrodynamic and chemical equilibrium model

Cyril Garneau[1], Sauvage S.[1] , Sánchez-Pérez J-M.[1], Lofts S.[2], Brito D.[3], Neves R.[3], Probst A.[1]

[1] ECOLAB, Université de Toulouse, CNRS, INPT, UPS, 31400 Toulouse, France

[2] NERC Centre for Ecology and Hydrology, Lancaster Environment Center, Bailrigg, Lancaster, LA1 4AP, U.K.

[3] Maretec, Instituto Superior Técnico, University of Lisbon. Av. Rovisco Pais 1049-001 Lisboa, Portugal

Abstract

Trace metals (TMs) in rivers experience a complex chemistry that affects their partitioning between the dissolved and particulate fractions. Predictive modelling of this partitioning is challenging, particularly under variable hydrodynamic conditions in rivers. This paper presents a coupled hydrodynamic–geochemical model for trace metal dynamics in rivers, to highlight key parameters and set a basis for developing simplified models. A coupled model based on the hydrodynamic model MOHID and the chemical speciation model WHAM was applied to the middle part of the Garonne River (SW-France). The predictions of the coupled model are compared to those of a fixed Kd partitioning model.

The model accurately simulates trace metal behaviour under varying hydrological conditions. The importance of the riverbed geomorphology and the diurnal variations in pH on TM concentrations in the water column are underlined. The sensitivity analysis ranked all physico-chemical parameters according to their influence on TM behavior.

Highlights:

- A hydrodynamic-geochemical model simulating trace metal (TM) in river was developed.
- TM behaviour was sensitive to the varying physico-chemistry of the water column.
- River morphology influenced the erosion and sedimentation zones of trace metals.
- The model suggested that diurnal cycle of pH strongly influences TM partitioning.
- Between 41 to 61% of Cu and 71 to 79% of Pb settled in the riverbed.

Keywords: MOHID, WHAM, Trace metal, partitioning coefficient, hydromorphology, Garonne River

1 Introduction

Rivers are a preferential pathway for solid and dissolved material export from continents to oceans. Therefore, they are susceptible to high input fluxes of pollutants from the watershed. One class of such

pollutants comprises the trace metal elements (TMs) which, in contrast to many other classes of pollutants, are highly persistent in sediments since they cannot be degraded and they provide a delayed source of contamination to the river by leaching and erosion. TMs are also a potential risk for human and ecosystem health (Oliver, 1997). In order to assess their toxicity, it is important to consider not only the dissolved concentration in the water (Caruso et al., 2008; Di Toro et al., 2001), but also the chemical speciation of the TMs. Furthermore, even if a significant fraction of complexed TMs is not readily bioavailable, these complexes can also react rapidly to changes in physicochemical conditions and act as a buffer on the free metal concentration (Di Toro et al., 2001).

Transport of TMs in river follows different pathways depending on physicochemical form. Dissolved and colloidal TMs are transported with the bulk water flow with a contribution of diffusion. The presence of transient storage zones, such as dead arms or the hyporheic zone, can induce more complex patterns of dispersion in the water column (Bencala and Walters, 1983; Bottacin-Busolin et al., 2011; Runkel et al., 1999). TMs bound to suspended particulate matter (SPM) are transported with the flow, but may also deposit to the riverbed. Deposited material may itself be subsequently eroded. The association of TMs and SPM varies a number of factors, including the chemical composition of the water and SPM. Detaching instream biofilm can generate particulate organic matter (Boulêtreau et al., 2006; Graba et al., 2012) while many sources of material, organic or mineral, can contribute to SPM loads via runoff erosion (Ludwig et al., 2005) or in-stream erosion (Allen et al., 1999). Overall, however, the organic matter content is often related to the SPM concentration of a river (Meybeck, 1982; Semhi, 1996; Veyssy et al., 1996) which, in turn, depends on the river hydrology (Oeurng et al., 2010; Probst and Bazerbachi, 1986; Semhi, 1996). Furthermore, complex river geometry may influence SPM dynamics. Successions of riffles and pools can, under specific hydrological conditions, lead to successive erosion and deposition zones (Garneau et al., 2015) while larger hydraulic obstacles such as dams and weirs, create high deposition zones.

The overall partitioning of TMs between the SPM and the water column, expressed as the partition coefficient (Kd), results from the chemical processes affecting TM speciation. The Kd has been extensively documented for most elements (Allison and Allison, 2005) and is, indeed, far from a constant: it varies depending on the chemical composition of the water and the SPM (Cao et al., 2006; Christensen and Christensen, 2000; Dai and Martin, 1995). The variation of the Kd should not be seen as resulting from a single geochemical process, but from a combination of simultaneous binding processes to ligands in the water and on the SPM. Weak binding includes electrostatic sorption (Drever, 1997), for example to fixed-charge clays. Specific binding to stronger adsorbents (e.g. carbonates, organic matter, iron or manganese oxides) can further reduce the mobility of TMs. This gradation of chemical strength between TMs and SPM can be identified by sequential extractions (Leleyter and Probst, 1999; Tessier et al., 1979)

Many different model frameworks can compute the chemical speciation of TMs such as PHREEQC (Parkhurst and Appelo, 1999), MINTEQA2 (Allison et al., 1991), CHESS (Santore and Driscoll, 1995) or WHAM (Tipping et al., 2011a) and thus in principle compute Kds as a function of the water chemistry. At

the opposite scale, models working at the river or watershed scale often use very simple partitioning models. The WASP model (Ambrose et al., 1993), for example, implements a fixed Kd while the SWAT model (Neitsch et al., 2009) considers TMs as inert tracers and simulates them by applying mass-balance relationships in the rivers.

Modelling the state of TMs (dissolved or particulate) in natural waters has been the objective of many studies. Complex chemical models have been applied to a wide range of situations, from groundwater quality assessment (Stigter et al., 1998; van Breukelen et al., 2003) to surface water geochemistry (Thorstenson and Parkhurst, 2002), acid mine drainage (Chapman et al., 1983) or to waters characterized by high concentrations of organic matter (Lofts and Tipping, 2000; Weng et al., 2002). These models are usually applied to laboratory experiments since they require a detailed description of the physico-chemistry of the water and of the SPM. One exception is the TICKET model (Farley et al., 2011, 2008) which uses the MINTEQA2 and WHAM V models in a spatial framework with slow dynamics to model chemical gradients (i.e. groundwater, sediment or lake models). Large scale applications have also been performed on samples from rivers (Ji et al., 2002; Lindenschmidt et al., 2006; Lofts and Tipping, 2000; Runkel et al., 1999), lakes (Cao et al., 2006; Farley et al., 2008) and at the soil – water interface (Almås et al., 2007; Shi et al., 2007) or the sediment – water interface (Caruso, 2004; Periáñez, 2004). The models used ranged from very simple fixed Kd to a complex representation of the variability of the Kd using speciation modelling.

Very few studies have attempted to study the detailed geochemistry of large rivers over long time scales (e.g. a year) to integrate varying hydrological conditions and to dynamically predict in-situ partitioning and fate of TMs. To our knowledge, even where regular and relevant measurements exist (Aubert et al., submitted; Davide et al., 2003; Sánchez-Pérez et al., 2006), no study has coupled complex geochemistry with physical processes such as hydrology and hydrodynamics. By coupling speciation and hydrodynamic models, it is possible in principle to dynamically describe TM geochemistry.

Considering the extensive experimental knowledge about the behaviour of TM in rivers and the limited modelling options to simulate TM sorption-desorption under varying hydrological conditions, the objective of this study was to simulate metal transport by coupling a chemical speciation model with a hydrodynamic model integrating heterogeneous morphology. The WHAM chemical model (Tipping et al., 2011a) and the MOHID hydrodynamic model (Trancoso et al., 2009) were chosen for their physical and conceptual bases. This MOHID – WHAM coupled model was compared with MOHID coupled to a fixed Kd sorption – desorption model. These two approaches were then used to a) evaluate the ability of the coupled model to simulate TM behaviour along a large river exhibiting variable hydrology and morphology, b) evaluate the influence of a variable Kd model on the predicted partitioning between dissolved and particulate phases and its influence on the transport of TMs and c) apply sensitivity analysis to the coupled model to highlight the key parameters and processes controlling the transfer and fate of TMs in a large river.

With the knowledge obtained by the complex coupled MOHID – WHAM model, it will then be possible to propose simpler conceptual models based around the parameters that exert the most influence in describing TM fate in rivers. The considered study site was the Garonne River in its middle course (South-West of France).

2 Material and Methods

The coupling of a hydrodynamic model and a chemical model was done in two steps. The first step was to setup the hydrodynamic model. Once the hydraulics, the transport of dissolved elements and the transport, erosion and sedimentation of SPM were calibrated, the chemical model of sorption – desorption was added to describe the behaviour of the TMs. Finally, a series of assumptions were made to provide input to the chemistry model. These assumptions are listed and justified for the case of the Garonne River.

2.1 The MOHID hydrodynamic environment

The hydrodynamic model was generated with the MOHID (http://www.mohid.com/) modelling framework written in FORTRAN 95. The River Network module (Trancoso et al., 2009) was used to simulate water flow and TM transport in the river. MOHID implements the full St-Venant equations in one dimension. A modelled river is thus discretized into nodes and reaches, allowing both temporal and spatial modelling. When available, the use of numerous river profiles allows for a fine description of the morphology of the river by describing the river profile and elevation at each node (Sauvage et al., 2003). Calculations are performed using a finite-volume approach and require the calibration of a single parameter, the Manning roughness coefficient, an empirical coefficient which depends on a number of factors such as the surface roughness or vegetation affecting the flow.

Two modules of MOHID were activated to transport TMs, namely the transport of suspended elements through advection – dispersion, and the erosion and deposition of SPM. Following Garneau et al. (2015), the transient storage model One-dimensional Transport and Input Storage (OTIS) was added to the River Network model (Bencala and Walters, 1983). OTIS is a conceptual model which considers a storage zone under the river. Exchanges between the river and the storage zone are strictly vertical and depend on two parameters, namely the exchange rate α (s^{-1}) and the cross section of the storage zone A_s (m^2). The variation of concentration in the river and the storage zone is driven by equations 1 and 2.

$$\frac{dC}{dt} = \alpha(C_s - C) \quad (1)$$

$$\frac{dC_s}{dt} = \alpha \frac{A}{A_s}(C - C_s) \quad (2)$$

where C and C_S (in mg.l^{-1}) are the concentrations of the dissolved element respectively in the river and in the storage zone, A and A_S (in m²) are the cross section of the river and the storage zone respectively and α (s^{-1}) is the exchange rate between the river and the storage zone.

The modelling of SPM concentrations is a critical issue for simulation of TMs. Furthermore, the SPM chemical composition and the physical characteristics during high flow could differ greatly from those during low flow (Bianchi et al., 2007; Hatten et al., 2012; Hedges et al., 1986; Veyssy et al., 1996). Therefore, SPM was modelled through four processes: transport by advection and dispersion, erosion and sedimentation. Two distinct classes of particles were used to simulate the heterogeneity of SPM with respect to erosion and sedimentation. The first class comprises "fine" SPM that was prone to sedimentation, and was input to the river system during high flow conditions. The second class comprises a "very fine" SPM fraction that exhibits very low settling velocity either because of its size or its density. This second class was included to provide the minimum SPM concentrations under low flow conditions. The two classes were modelled by equations derived from the Partheniades (1965) model with class–specific parameters (critical shear stress for deposition and erosion, settling velocity, erosion constant; see Trancoso et al., 2009).

The dynamics of the particulate–associated component of the TMs was assumed to be the same as that of the SPM fraction to which it was bound. Therefore, particulate TMs were also considered in two classes that possessed exactly the same erosion and sedimentation parameters as the SPM, with the exception of the erosion constant. Eroded sediment was assumed to have a constant concentration of TMs (g.g^{-1}) throughout the river network. Therefore, the erosion constant of the TMs was defined as the erosion constant of the associated SPM class multiplied by the concentration of the TMs in the sediment:

$$e_{TMs} = e_{SPM} \times C_{TMs\ in\ river\ bed\ sediment} \quad 3$$

where e_{TMs} is the erosion rate of the TM in kg.m^{-2}.s^{-1}, e_{SPM} is the erosion rate of the SPM in kg.m^{-2}.s^{-1} and $C_{TMs\ in\ river\ bed\ sediment}$ is the concentration of the TMs in the river bed sediment in g.g^{-1}.

Finally, MOHID allows computation of SPM and particulate TM accumulation on the riverbed by computing the difference between the initial and final mass of SPM or TM in a given reach on each timestep. Therefore, two outputs were obtained: the accumulated mass per meter of river and the total accumulated mass within the full river sector.

2.2 The fixed Kd implementation

A fixed Kd partitioning model was used as a benchmark to quantify the importance of the dynamic physico-chemical model. It was coupled to the MOHID model and is referenced as the MOHID – Fixed Kd model. The fixed Kd model required one parameter per TM (the Kd), and computed the equilibrium between dissolved and particulate phases directly, without the underlying complex chemistry. Therefore, equation 4 was used and the Kd was taken as a fixed parameter instead of a variable one:

$$Kd = \frac{TM_{SPM\,part}}{TM_{diss}} \quad (4)$$

Where Kd is the partition coefficient (l.kg^{-1}), $TM_{SPM\,part}$ is the particulate concentration of TM per kilogram of SPM (µg.kg^{-1}) and TM_{diss} is the dissolved concentration of TM (µg.l^{-1}).

2.3 The WHAM implementation

The Windermere Humic Aqueous Model (WHAM) is a model for the prediction of equilibrium speciation in natural environments. WHAM has a particular emphasis on the ion-binding reactions of natural organic matter and mineral oxide surfaces. It takes as inputs the sum of the dissolved and the labile particulate concentration of TMs, the concentration of the adsorbent and the physico-chemistry of the water, and returns predicted concentrations of dissolved and labile TMs. The reader must refer to the supplementary material and to Tipping (1994), Lofts and Tipping (1998), Tipping et al. (2011b) for a comprehensive mathematical formulation of the model.

The labile particulate concentration of metal refers to the particle–associated metal that is chemically reactive and which is assumed to be capable of exchanging with the dissolved metal on short timescales. It may be estimated by a partial extraction of metal from SPM, for example by acidification (Neal et al., 1997).

WHAM includes submodels for ion binding to humic substances, to mineral oxide surfaces and to a fixed-charge cation exchanger. The model also requires concentrations of major ions (Na, Ca, Fe, Al, Mg, K, Cl, NO_3), the main physico-chemical parameters of the water (pH, CO_2 partial pressure, temperature) and the concentration of the TMs (sum of dissolved and labile particulate concentrations) to be modelled.

2.4 Coupling of the chemical model to the hydrodynamic model

The coupling between WHAM and MOHID was done by a direct implementation of WHAM in the MOHID code. Since the MOHID model is written in ANSI FORTRAN 95, the WHAM model was recoded to ANSI FORTRAN 95 as well. In the scope of MOHID, the sorption-desorption process was added as a source-sink process between the dissolved and the particulate phase of a metal. MOHID is thus a 1D river model and WHAM is a 0D model which is applied to every cell of the discretized river.

MOHID simulates a TMs transport under two fractions: dissolved and total particulate. The WHAM model computes the partitioning of the labile metal (comprising dissolved and labile particulate). Computation of Kd for total metal from the Kd computed by WHAM (Kd_{labile}) was done by considering the fraction of total particulate that is not labile (the residual fraction):

$$Kd_{labile} = \frac{TM_{SPM\,labile}}{TM_{diss}} \quad (5)$$

$$Kd = \frac{TM_{SPM\,part}}{TM_{diss}}$$

$$= \frac{TM_{SPM\,labile} + TM_{SPM_{residual}}}{TM_{diss}} \quad (6)$$

$$= Kd_{labile} + \frac{TM_{SPM_{residual}}}{TM_{diss}}$$

where $TM_{SPM\,labile}$ and $TM_{SPM_{residual}}$ are the concentrations of TM in the particulate labile and residual forms. The proportions of labile and residual particulate metal were expressed as a proportion of the total:

$$TM_{residual} = f_{res} \times TM_{part} \quad (7)$$

$$TM_{labile} = (1 - f_{res}) \times TM_{part} \quad (8)$$

where f_{res} is the fraction of residual TM in the particulate fraction. In terms of Kds:

$$Kd = \frac{Kd_{labile}}{1 - f_{res}} \quad (9)$$

The output of WHAM is the Kd_{labile} on which are updated the concentration of dissolved and labile TM. The updated dissolved concentration of TM is provided as is to the MOHID model and the full particulate fraction of TM is reconstructed by adding the residual concentration to the new labile concentration of TM.

The computation of the new equilibrium can quickly become the most computationally intensive part of the simulation. Therefore, a criterion was defined to decide whether or not the Kd should be updated. Since the two most influential inputs to the model were the concentration of SPM and the pH, it was decided to recompute Kd only if the SPM concentration or the pH in a cell of the model varied by more than a predefined threshold. Otherwise, the Kd computed for the cell on the previous timestep was reused. This solution provided a very detailed evolution of the Kd under changing hydrological conditions and under the diurnal variation of the pH, but prevented excessive computations when the chemical conditions were stable. In the scope of these works, the threshold was defined as a variation of the SPM by more than 8% from the last calculation or a variation of more than 2% of the pH. These thresholds allowed reduced computational time with limited influence on the simulation results.

2.5 Study site description

The Garonne River (South-West of France) is the third largest river of France and is eighth order at its mouth. It exhibits a nivo-pluvial regime with the influence of the winter snow precipitation in the

Pyrenean Mountains at its inlet (Pardé, 1935) . Figure 1 – (a) shows the extent of the Garonne River from the southern part of France to its outlet, in the West. The study site is the middle course of the Garonne along an 87 km reach that passes the city of Toulouse (800 000 inhabitants) (Figure 1 – (b)). The downstream limit of the study site is above the Malause dam. The daily flow of the Garonne River is well monitored at the Verdun gauging station, in the middle part of the study site (G5 on Figure 1 – (b)). At this point, the Garonne has a watershed of 13 730 km^2 and an annual average flow of 193 $m^3.s^{-1}$. The monthly average flow ranges from 75 $m^3.s^{-1}$ in August to 341 $m^3.s^{-1}$ in May. The 10 day low flow average with a return period of two years is 42 $m^3.s^{-1}$ while the daily average flow of the two years return high flow reaches 1400 $m^3.s^{-1}$ (Banque Hydro, http://www.hydro.eaufrance.fr/). In this context, the year 2005, used for the simulations, was dry, with an annual flow of 158 $m^3.s^{-1}$. Furthermore, the largest daily flow recorded reached 800 $m^3.s^{-1}$, far from the two years return high flow of 1400 $m^3.s^{-1}$.

The Garonne River at Toulouse is impacted by three dams and eight bridges before the sampling point G1, providing a complex hydraulic behaviour (S.M.E.P.A.G., 1989). Then, downstream of Toulouse, the river exhibits successions of riffles and pools (Steiger and Gurnell, 2003). This morphological characteristic means that successive erosion and sedimentation zones can be observed in the 87 km reach of the study. In addition, an important gravel bed can be observed which is known to generate important interactions between the river and the groundwater for phosphorus and nitrate (Bonvallet Garay et al., 2001; Garay et al., 2001; Teissier et al., 2008).

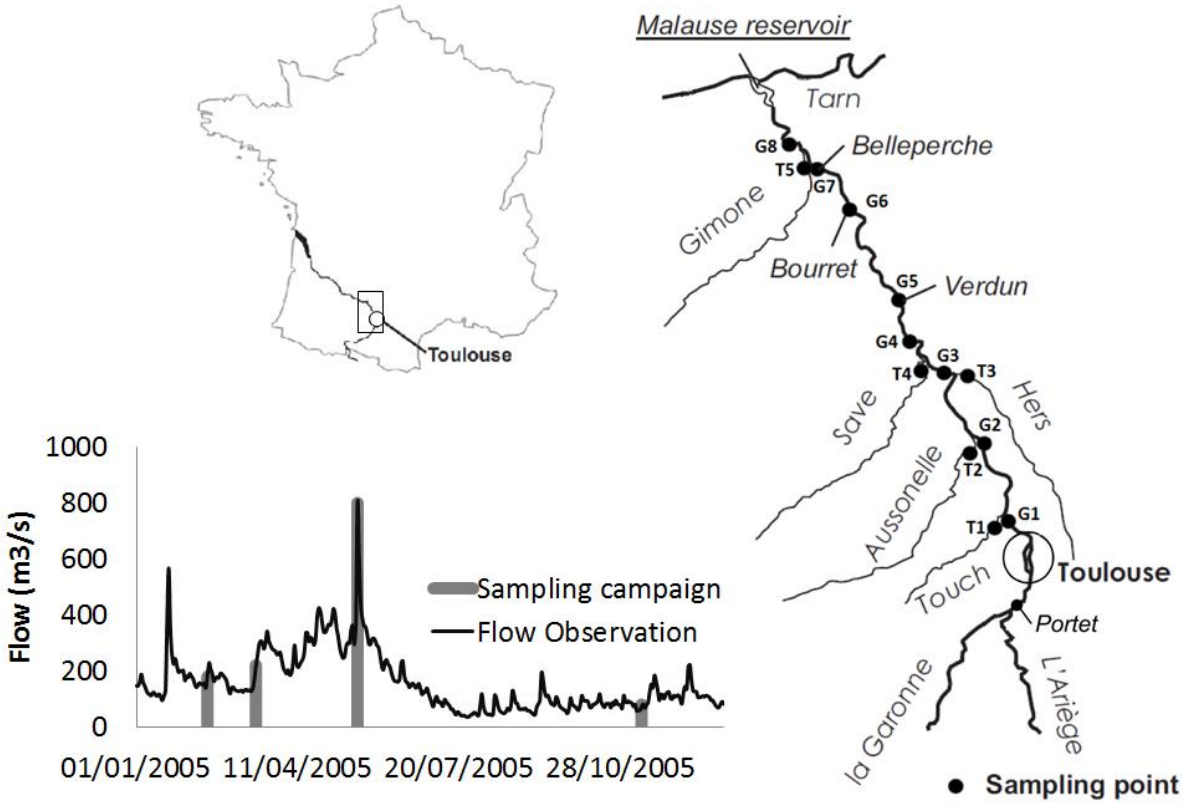

Figure 1: The Garonne River study site in the South-West of France. The model was applied over the Garonne river section between Portet (upstream Toulouse city) and station G8 (upstream the Malause reservoir before the confluence with the Tarn river) for a total reach of 87 km. The sampling sites in Garonne main channel are indicated by "Gx" symbols and the tributaries sampled by "Tx" symbols. The hydrology of the sampling campaigns is also represented and was observed at the sampling point G5.

2.6 Available datasets

2.6.1 Hydrodynamic and morphologic data

Three different datasets were used to calibrate each sub-model independently (hydraulics, transport, erosion and sedimentation), thus preventing compensation among the different processes. The morphology of the river was assessed by more than 200 cross-sectional profiles along the reach gathered at various public institutions such as the Direction Départementale de l'Équipement (DDE – Departmental Office of Infrastructures) or the Direction Régionale de l'Environnement (DIREN – Regional Department for the Environment). These profiles, separated by a distance ranging from 30 m around bridges to a maximum of 2.4 km, allowed a fine scale description of the river slope and cross-section to be provided to the model. A trapezoidal approximation of the true profiles was used.

Water velocity requires high frequency flow to be properly described. However, limited hourly flow time series were available, including a gap during the period of sampling the TMs (see below). Therefore, it was decided to use two datasets: one for the calibration – validation of the hydrodynamics and a second one for the TM simulations.

The dataset for calibration – validation consisted of hourly flow data at the Portet gauging station (upstream of Toulouse) and at the Verdun gauging station(sampling point G5, Figure 1). The water level was measured and converted to discharge by the Direction Régionale de l'Environnement, de l'Aménagement et du Logement – Midi-Pyrénées (DREAL, http://www.midi-pyrenees.developpement-durable.gouv.fr/). Calibration of the Manning coefficient was performed with hourly data from 07/02/2002 to 19/02/2002 and validation was done with the observations for the period 29/03/2002 to 08/03/2002. This calibration was performed by Garneau et al. (2015) and aimed to maximize the Nash-Sutcliff efficiency index (equation 10).

$$NS = 1 - \frac{\sum(Q_{obs} - Q_{sim})^2}{\sum(Q_{obs} - \overline{Q_{obs}})^2} \qquad 10$$

Where Q_{obs} is the observed flow, $\overline{Q_{obs}}$ is the average observed flow and Q_{sim} is the simulated flow.

The dataset for simulation of the TMs consisted of daily average flows. These daily data were used to provide the input flow at the Portet station (Figure 1). The downstream boundary condition was provided by the dam at the outlet of the Malause reservoir (Figure 1) which operates at a fixed water level.

The transport equations (advection – dispersion and transient storage) were calibrated as reported in Garneau et al. (2015). Three parameters (diffusivity, the exchange rate α and the cross section of the

transient storage zone A_S) were calibrated by minimizing the root mean square error between the simulation and the observations.

2.6.2 Temperature, pH and turbidity observations

The Conseil Général de la Haute-Garonne (General Council of Haute-Garonne, http://labo-eau.haute-garonne.fr/) monitors the temperature, the pH and the turbidity (in Nephelometric Turbid Units (NTU)) of the Garonne River in real-time (average time step of 24 minutes) at Portet station (Figure 1). During the year 2005, the water temperature ranged from 2.6 to 25.8 °C with an average temperature of 15.4 °C. The pH ranged from 7.2 to 9.2 with an average of 8.1 and the turbidity ranged from 2 to 302 NTU with an average turbidity of 10.2 NTU. The relationship between turbidity and SPM measured in the Garonne River have been modelled empirically by Probst J.L., Probst A. and Aubert D. (personal communication) on the basis of turbidity – SPM measurements performed in numerous studies (Etchanchu, 1988; Probst, 1983; Probst and Bazerbachi, 1986; Semhi, 1996) corresponding to variable hydrological conditions. These SPM calculated using the turbidity measures were used as the input variable to the model (equation 11, n = 336, $R^2 = 0.95$, $p < 0.001$).

$$SPM = 13027 \times (e^{1.362E-4 \times T} - 1) \quad 11$$

where the SPM are in $mg.l^{-1}$ and T is the turbidity (NTU).

2.6.3 Suspended particulate matter and trace metal data

Four sampling campaigns were performed in 2005 to measure the total SPM and TM on the Garonne River and its tributaries (Sánchez-Pérez et al., 2006). The sampling points of the Garonne (G_i) and its tributaries (T_i) are shown on Figure 1 and were sampled from the first sampling point (upstream) to the last (downstream) at the velocity of the river flow according to the method of Teissier et al. (2008). Furthermore, the "Système d'Information sur l'Eau du Bassin Adour-Garonne" (SIE, translated as "Water Information Network of the Adour-Garonne watershed", http://adour-garonne.eaufrance.fr/) collected monthly SPM data at three sampling points (G1, G5 and G8).

In the scope of this work, we chose two metals, copper (Cu) and lead (Pb), which are characterized by contrasted sorption/desorption behaviour. The first one (Cu) exhibits a significant dissolved fraction whereas Pb is transported mainly in particulate form (Aubert et al., submitted; Brunel et al., 2003; Sánchez-Pérez et al., 2006; Tipping et al., 2003).

The first campaign took place on 14 February 2005, during a snow melt event with a flow of 187 $m^3.s^{-1}$. The second was on 16 March 2005, after one month without a significant hydrological event, with a flow of 218 $m^3.s^{-1}$. The third was on the 17 May 2005 and 18 May 2005 during high flow (up to 800 $m^3.s^{-1}$). Finally, the fourth campaign took place on the 10 October 2005 after three weeks of low flow conditions (80 $m^3.s^{-1}$, see Figure 1). In total, 43 samples were taken from the Garonne River. The partition coefficients between the dissolved and particulate phases of Cu and Pb are shown in Table 1. The calculated Kd

showed a large variability within the range, as shown by the standard deviation of the log-transformed Kd.

Table 1: Statistics on the separation coefficient (particulate / dissolved) Kd calculated from the 43 samples taken during the four sampling campaigns. The $\log_{10}$ (Kd) was used for easier reading. An important variability in the values of Kd was observed, as suggested by the standard deviation of the log-transformed Kd.

	Log_{10} (Kd min)	Log_{10} (Kd max)	Log_{10} (Kd average)	$\sigma(\text{Log}_{10}\, Kd)$
Cu	4.4	5.0	4.7	0.13
Pb	5.4	6.7	6.3	0.33

A distinct sampling campaign was performed during 2002, upstream of Toulouse city, with the same sampling protocol. A total of 44 weekly samples over the full year were taken in the Garonne River and its main affluent, the Ariège River (see Figure 1). Dissolved and particulate TMs were analysed along with physico-chemical parameters (Aubert et al., submitted).

Sixteen SPM observations made during the campaigns of May and October 2005 were used to calibrate the erosion – sedimentation model according to the calibration procedure used by Garneau et al. (2015). This procedure allowed for a spatially well resolved description of the SPM with respect to the morphology of the river. The parameter set obtained was validated at three sampling sites (G1, G5 and G8) using the data of the two remaining sampling campaigns as well as the data collected by the SIE, for a total of 14 observations per sampling site. This validation procedure assesses the performance of the erosion – sedimentation model in space, as the sampling sites are close to the inlet, in the middle and close to the outlet of the modelled river. It also assesses its performance under various hydrological conditions as time series at each sites are generated. The Mean Absolute Error (equation 12) and the correlation coefficient (equation 13) were used to assess the validity of the parameters.

$$MAE = \frac{\sum|Obs_i - Sim_i|}{n} \quad 12$$

$$r = \frac{\sigma_{Obs,Sim}}{\sigma_{Obs}\sigma_{Sim}} \quad 13$$

2.7 Physico-chemical inputs

The WHAM model requires a large number of chemical variables to compute the Kd. Since the majority of these variables are not routinely measured, a number of assumptions needed to be made. The exceptions were pH and water temperature, for which suitable time series data were available.

2.7.1 Trace metal inputs (dissolved and particulate)

In absence of TM time series, empirical relationships were built based on the dataset of Aubert et al. (submitted) to estimate the concentrations of Cu and Pb at the upstream boundary of the modelled sector (Table 2). Dissolved Pb was correlated to flow (r = 0.49, n = 37, p = 0.002) and particulate Pb was correlated

to SPM (r = -0.66, n = 12, p = 0.019). Dissolved and particulate Cu, in the other hand, were not significantly correlated to flow or SPM. It was therefore decided to fix their values to the average concentrations observed at Portet during the 2005 campaign. Finally, the riverbed acts as a secondary source and sink of TM through sedimentation and erosion (Audry et al., 2004; Brunel et al., 2003). The total TM concentrations in riverbed sediments were estimated based on previous works on the Garonne River (Garneau et al., 2015), expert knowledge (Probst, A., Aubert D. and Probst J.L., personal communication) and data collected by the DREAL. The residual fraction was estimated based on sequential extraction experiments performed on SPM and sediments of similar compositions (Probst et al., 2003; Roussiez et al., 2013).

Table 2: Hypothesis on the dissolved and particulate concentrations of Cu and Pb at the upstream of the river, the Cu and Pb concentration in the sediment and on the residual fraction of Cu and Pb in the SPM (Aubert et al. (submitted) and unpublished data).

	Dissolved (µg.l^{-1})	Particulate (µg.g^{-1})	Residual fraction	Sediment (µg.g^{-1})
Pb	$0.0014 \times Q^{0.4635}$	$131.17 \times SPM^{0.7997}$	0.80	7.0
Cu	0.547	40.0	0.50	7.0

2.7.2 SPM characterization (OM, metal oxides, clays)

The SPM content estimated from the NTU observations was separated into two classes, “very fine” and “fine”. The very fine size fraction was assumed to comprise all the SPM during low flow conditions. The “fine” SPM represented coarser sediment eroded from the watershed under elevated flow conditions. Probst and Bazerbachi (1986) demonstrated that the average SPM concentration in the Garonne during low flow is 5.3 mg.l^{-1}. Therefore, the upstream concentration of “very fine” SPM was fixed to 5.3 mg.l^{-1} and the remaining upstream SPM (calculated from equation 11) was assigned to be “fine” SPM.

WHAM allows the chemically reactive portion of the SPM to be composed of organic matter (humic and/or fulvic acid), oxides of iron, manganese, aluminium and silicon, and a fixed charge clay. Here we partly followed the schema of Lofts and Tipping (2000), who represented SPM using humic and fulvic acids and iron and manganese oxides, and also estimated SPM clay content. The concentrations of humic and fulvic acids were each assumed to be 50% of the particulate organic carbon (POC) . The concentration of particulate organic carbon (POC) has been related to the total concentration of SPM in various studies (Boithias et al., 2014; Ludwig et al., 1996; Meybeck, 1982; Veyssy et al., 1996). According to Veyssy et al. (1996), the POC never exceeded 24% of the SPM concentration in the Garonne River. Probst (1992) and Boithias et al. (2014) expressed the fraction of POC to the total SPM concentration through equation 14.

$$f_{POC} = \frac{NUM}{SPM - SPM_{Min}} + f_{POC_{Min}} \qquad 14$$

Where $f_{POC_{Min}}$ is the minimum fraction of POC in the SPM. Its value tends to the average POC content in the watershed soil (mg.mg^{-1}), SPM_{Min} sets the asymptotic limit of the relationship between f_{POC} and the

SPM concentration (mg.l^{-1}). Equation 14 is thus valid only when $SPM > SPM_{Min}$. The numerator NUM is catchment specific and describes the change of origin of POC from autochthonous production to watershed export as the SPM concentration raises (mg.l^{-1}).

The $f_{POC_{Min}}$ value was fixed to 0.021 based on literature on the Garonne River watershed (Probst, 1983; Veyssy et al., 1996) while the values of NUM and SPM_{Min} were set to 0.60 and 1.0 based on the POC and SPM observations of the sampling campaigns of 2005. The full equation is reported in Table 3.

Iron content measured in the SPM during the sampling campaigns indicated that iron composed between 1% and 7% of the total SPM with an average of 3%. This value of 3% was used as a constant ratio of iron oxide in the SPM. The concentration of the manganese oxide was determined in the same way and was fixed to 0.1% of the SPM. Finally, the clay content was fixed at 50% of the remaining SPM, based on the work of Semhi (1996) on the Garonne River. The different hypotheses are summarised in Table 3.

Table 3 : Fractionation of the SPM in its different constituents. The percentage of POC varies with the inverse of the SPM concentration while the percentages of iron and manganese oxides are fixed. The clays comprise 50% of the remaining SPM. The humic and fulvic acid concentrations are fixed at 50% of the POC. The concentration of each phase is then provided to WHAM to compute the Kd_{labile} of each TM.

	Fractions observed
Particulate organic carbon	$f_{POC} = \min\left(\frac{0.60}{SPM - 1.0} + 0.021, \quad 0.24\right)$
Humic acid	$f_{HA} = 0.5 \times f_{POC}$
Fulvic acid	$f_{FA} = 0.5 \times f_{POC}$
Iron oxide	$f_{FeOx} = 0.03$
Manganese oxide	$f_{MnOx} = 0.001$
Clays	$f_{Clay} = 0.50 \times (1 - f_{POC} - f_{FeOx} - f_{MnOx})$

2.7.3 Physico-chemistry and major ion concentrations

Major ion and dissolved organic carbon (DOC) concentrations are required by the WHAM model to compute the activity of the various chemical complexes. These elements all exhibit specific travel paths and are under the influence of different processes which can be simple, such as dilution, or very complex such as those linked to the biogeochemistry of nitrogen. Therefore, the concentrations of the major ions were fixed to the average concentrations observed during the 2005 sampling campaign over the eight sampling sites. The concentration of DOC was estimated similarly. For modelling, the DOC concentration was converted to a fulvic acid concentration by multiplying it by 1.3 (Bryan et al., 2002) The concentration of carbonate was modelled by specifying the partial pressure of CO_2, based on the work of Semhi et al. (2000a) and fixed to 1680 ppm (Table 4). This partial pressure is equivalent to an alkalinity of 3.3 mmol.l^{-1}, which is in the range of the observed alkalinity on the Garonne River (from 1 mmol.l^{-1} to 5.3 mmol.l^{-1}).

Table 4: Average concentrations of major ions and physico-chemical parameters measured during the 2005 campaign in the Garonne River at the eight stations (PCO2 from Semhi (1996) and Semhi et al. (2000a)). These data were used as constant inputs for the WHAM Model.

Ion concentration ($\mu g.l^{-1}$)	
K^+	2700
NO_3^-	12000
Na^+	1243
Ca^{+2}	46800
Mg^{+2}	6290
SO_4^{-2}	24163
Cl^-	16010
Al^{+3}	9.3
Fe^{+3}	118
Physico-chemical parameters	
Dissolved organic carbon ($mg.l^{-1}$)	1.87
pCO_2 (ppm)	1680

2.7.4 Fixed Kd hypothesis

The simulation results of the dynamic Kd were compared to those observed with a fixed Kd. For each TM, two different values of fixed Kd were tested to explore the range of possible strength of particle binding: the minimal and maximal observed Kd during the sampling campaigns of 2005. This choice generated maximal variation in the TM partitioning.

Table 5: Values of Kd used for the fixed Kd scenarios. The Kd values were calculated during the sampling campaign of 2005 (Aubert et al. unpublished data). Only the minimal and maximal values were used in the simulations of the fixed Kd scenario.

	Minimum log10 (Kd)	Maximum log10 (Kd)
Pb	5.4	6.7
Cu	4.4	5.0

2.8 Sensitivity analysis

A sensitivity analysis was performed on the MOHID – WHAM coupled model to identify the influence of the various parameters on the average Kd simulated and on its dispersion over time. The Latin Hypercube – One-at-a-Time (LH-OAT) method developed by van Griensven et al. (2006) was applied to the model.

The LH-OAT method screens the global parameter space with a Latin hypercube sampling. For each parameter set, the sensitivity of the model to each factor was estimated by the elementary effect calculated by eq. 15.

$$EE_{\theta,x} = \frac{\partial F_\theta}{\partial x} \quad (15)$$

Where $EE_{\theta,x}$, is the elementary effect of the parameter x for the parameter set θ and $\frac{\partial F_\theta}{\partial x}$ is the partial derivative of the score with respect to the transformed factor x evaluated by finite differences.

A total of 100 parameter sets were sampled by the LH sampling procedure and, to assess the spatial variation of the river, the elementary effects were computed at each sampling points (from G1 to G8, Figure 1). The simulation ranged from 1st of May until 1st of August to include high and low flows. The sensitivity analysis was performed with a constant pH. This hypothesis was made necessary by the large computer time required by the sensitivity analysis. Table 1 lists the 34 factors that were perturbed during the sensitivity analysis. The sampling of the parameter set was performed with a uniform distribution between the indicated minimum and maximum values. When a parameter was allowed to vary over many orders of magnitude, the logarithm of the parameter was sampled in a uniform distribution. The column "log" indicates whether (1) or not (0) the logarithm of the parameter was taken. Finally, to eliminate the influence of the units on the elementary effect, all parameters were standardized by removing their average and dividing by their standard deviation. Parameter ranges were estimated based on the published literature for the Garonne river (Probst, 1983; Probst and Bazerbachi, 1986; Semhi, 1996) and on the publications relative to various models (Garneau, 2014).

Table 6: List of parameters with their minimum and maximum value used in the sensitivity analysis. A "0" in the log column means that the sampling was performed between the Min and Max values of the factor while "1" means that the sampling was performed between log(Min) and log(Max) to effectively cover the large magnitude involved.

	No.	Factor	Units	Min	Max	log	Parameter description
Hydrodynamic and transport	1	Manning	$s.m^{-1/3}$	0.01	0.04	0	Manning coefficient representing the roughness of the channel.
	2	Diffusivity	$m^2.s^{-1}$	1.0E-7	3.0E+1	1	Dispersion parameter
	3	α	(adim)	1.0E-6	1.0E-3	1	Exchange rate between the river and the transient storage zone
	4	A_S	m^2	10	130	0	Cross-section of the transient storage zone
Erosion and sedimentation	5	$TM_{sedimer}$	$g.g^{-1}$	1.0E-8	3.0E-3	1	TM concentration in the sediment
	6	$\tau_{ero\ 1}$	Pa	8	15	0	Erosion critical shear stress for SPM - Class 1
	7	E_1	$g.m^{-2}$	1.0E-6	1.0E-4	1	Erosion constant for SPM – Class 1
	8	$W_{C\ 1}$	$m.s^{-1}$	1.0E-5	1.0E-3	1	Settling velocity for SPM – Class 1
	9	$\tau_{sed\ 1}$	Pa	0.1	8	0	Sedimentation critical shear stress for SPM – Class 1
	10	$\tau_{ero\ 2}$	Pa	20	60	0	Erosion critical shear stress for SPM – Class 2
	11	E_2	$g.m^{-2}$	1.0E-6	1.0E-3	1	Erosion constant for SPM – Class 2
	12	$W_{C\ 2}$	$m.s^{-1}$	1.0E-6	1.0E-3	1	Settling velocity for SPM – Class 2
	13	$\tau_{sed\ 2}$	Pa	10	20	0	Sedimentation critical shear stress for SPM – Class 2
SPM separation	14	f_{HA}	(adim)	0.1	0.9	0	Humic acid fraction in organic carbon
	15	f_{FeOH}	%	0.01	0.1	0	Iron oxide fraction in SPM
	16	NUM	(adim)	8	200	0	Numerator for the calculation of POC in SPM
	17	SPM_{Min}	(adim)	0.5	5	0	Parameter for the calculation of POC in SPM
	18	$f_{POC_{Min}}$	%	0.2	5	0	Minimum fraction of POC in SPM
	19	f_{clay}	%	0.1	1	0	Clay fraction in SPM
	20	f_{MnHx}	%	1.0E-4	1.0E-2	1	Manganese oxide fraction in SPM
Water chemistry	21	[DOC]	$mg.l^{-1}$	0.5	5.0	0	DOC concentration in water
	22	F_{res}	(adim)	0.2	0.8	0	TM residual fraction in SPM
	23	[Na]	$mg.l^{-1}$	3	66	0	Sodium concentration in water
	24	[Mg]	$mg.l^{-1}$	1.0E-3	8	0	Magnesium concentration in water
	25	[Al]	$mg.l^{-1}$	1.3E-4	3.8E-2	0	Aluminium concentration in water
	26	[K]	$mg.l^{-1}$	0.6	3.6	0	Potassium concentration in water
	27	[Ca]	$mg.l^{-1}$	10	73.5	0	Calcium concentration in water
	28	[Fe]	$mg.l^{-1}$	0.05	0.415	0	Iron concentration in water
	29	[Cl]	$mg.l^{-1}$	3	65	0	Chloride concentration in water
	30	$[NO_3]$	$mg.l^{-1}$	1	60	0	Nitrate concentration in water
	31	$[SO_4]$	$mg.l^{-1}$	6	75	0	Sulfate concentration in water

	32	pH	(adim)	6	9	0	Water pH
	33	pCO2	ppm	600	1600	0	CO_2 pressure in water
	34	ΔT	Kelvin	-2	2	0	Temperature variation

Two scores were computed to assess the sensitivity of the parameters: the average hourly Kd and the dispersion of the hourly Kd calculated by its standard deviation over the whole simulation. The influence of a parameter on the model was assessed by the average of the absolute value of the elementary effects.

$$\mu^* = \frac{1}{n}\sum_{\theta=1:n} \left|EE_{\theta,x}\right| \qquad 16$$

According to the method of van Griensven et al. (2006), the parameters were sorted from the most to the least influent at all sampling points (see Figure 1). The global score of a parameter was taken as the highest rank it achieved. Parameters of rank 1 were considered very influent. Parameters of rank 2 to 4 were considered influent and parameters of rank 5 to 34 were considered not influent.

3 Results

The simulation of a full year took 5 hours 24 minutes on an Intel Xeon CPU running at 2.66 Ghz for the MOHID – WHAM model.

3.1 Simulations of water flow and SPM content using the MOHID model

The calibrated parameters for the hydraulic, hydrodynamic and SPM model are shown in Table 7.

Table 7: Hydrodynamic and SPM parameters for the study case of the Garonne River

Hydrodynamic parameters	Value	
Manning coefficient ($s.m^{-1/3}$)	0.02	
Diffusivity ($m^2.s^{-1}$)	0.039	
α (s^{-1})	1.2e-4	
As (m^2)	34.0	
SPM model parameters	Class 1	Class 2
τ_{sed} (Pa)	4.8	16.8
τ_{ero} (Pa)	12.4	45.4
Settling velocity ($m.s^{-1}$)	4.2e-5	8.0e-4
Erosion constant ($kg.m^{-2}.s^{-1}$)	4.4e-6	6.0e-5

The flow simulated by the hydrodynamic model was compared to the observations at Verdun gauging station (sampling site G5 of the Garonne, see Figure 1). The SPM model was validated at three sampling stations, namely the point G1, G5 and G8 (Figure 2).

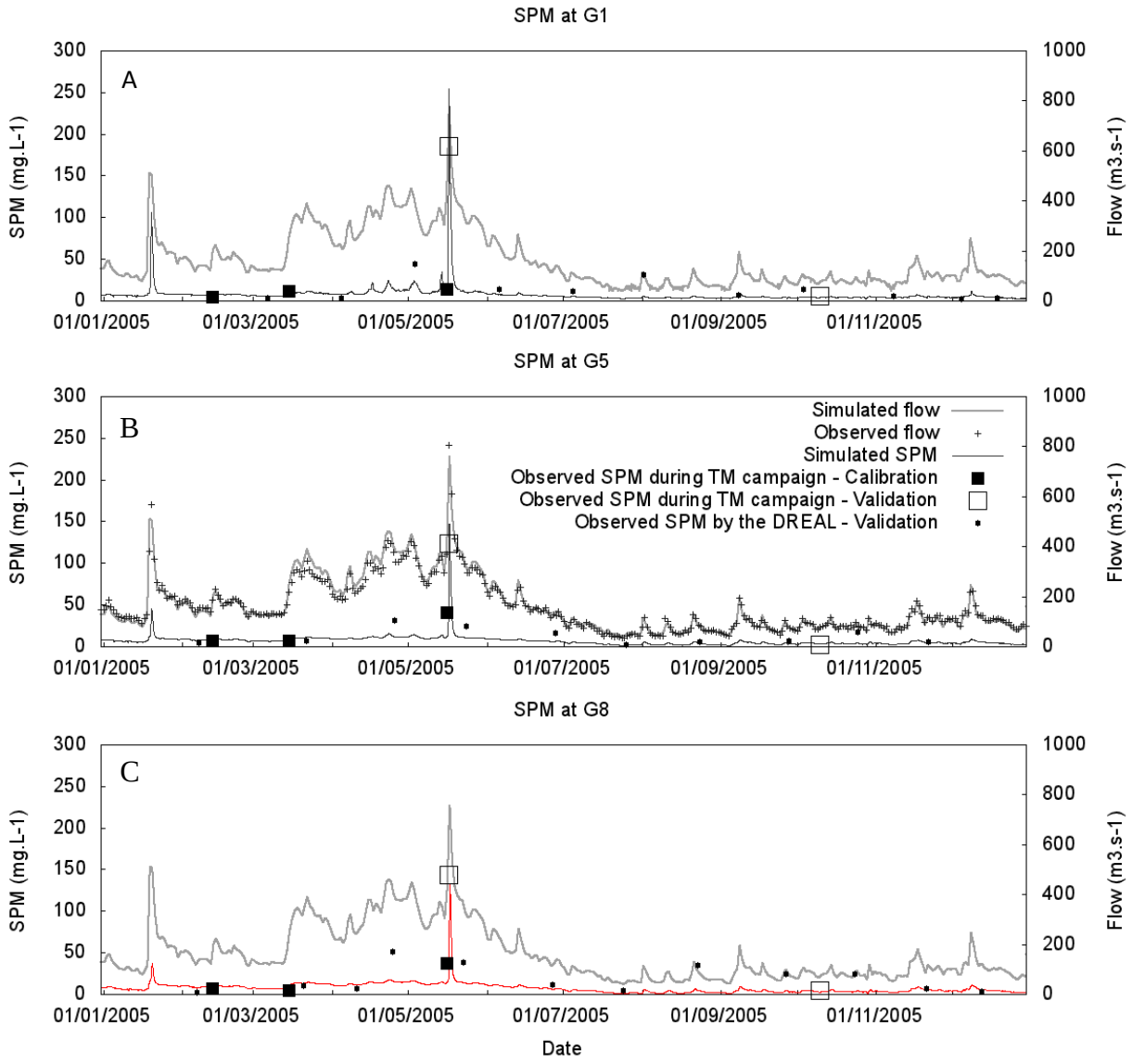

Figure 2: The simulated trends of SPM and discharge are shown for sampling point G1 (A), G5 (B) and G8 (C) (see Figure 1)) for the year 2005. The observed SPM refer to the sampling campaigns while the observed SPM DREAL are relative to data collected by the water agency DREAL (see section 2.6.3). The observed flows are presented at G5 (dotted) with the simulated flow to validate the hydrodynamic model. There are 27 km from the inlet of the model to point G1, 54 km to the sampling point G5 and 83 km to the sampling point G8.

The Nash-Sutcliff and the r relative to the hydrodynamics were calculated in Garneau et al. (2015) and were close to one: NS = 0.82, r = 0.98 for calibration and NS = 0.96 and r = 0.97 for the validation period based on hourly observations. The scores related to the daily data presented in Figure 2 were also very close to one (NS = 0.97, r = 0.99). These high values could be explained by the use of the mean daily discharge rather than hourly observations.

The MAE of the SPM simulations during the validation were of 6.6 $mg.l^{-1}$ at sampling point G1, 8.1 $mg.l^{-1}$ at G5 and 12.5 $mg.l^{-1}$ at G8. The corresponding scores were r = 0.72 at G1 (n = 14, p = 0.004), 0.60 at G5

(n = 12, p = 0.04) and 0.46 at G8 (n = 14, p = 0.09), respectively. Both the MAE and the r scores were decreasing as the sampling point got farther from the inlet. However, since the correlation between measured and observed data was good along the full sector, the parameter set obtained was deemed acceptable for the simulation purpose.

3.2 Simulations Cu and Pb by the MOHID – WHAM coupled model

The simulation predicted a strong influence of the hydrology on Cu concentrations (Figure 3). The two largest hydrological events (in January and May) generated high concentrations of particulate Cu. The model suggests that the high particulate concentration of Cu entering the system in January was mostly lost by sediment settling, while the May event contributed significantly to particulate Cu export from the river. In general, the concentration of particulate Cu followed a very similar trend to the SPM (shown in Figure 2).

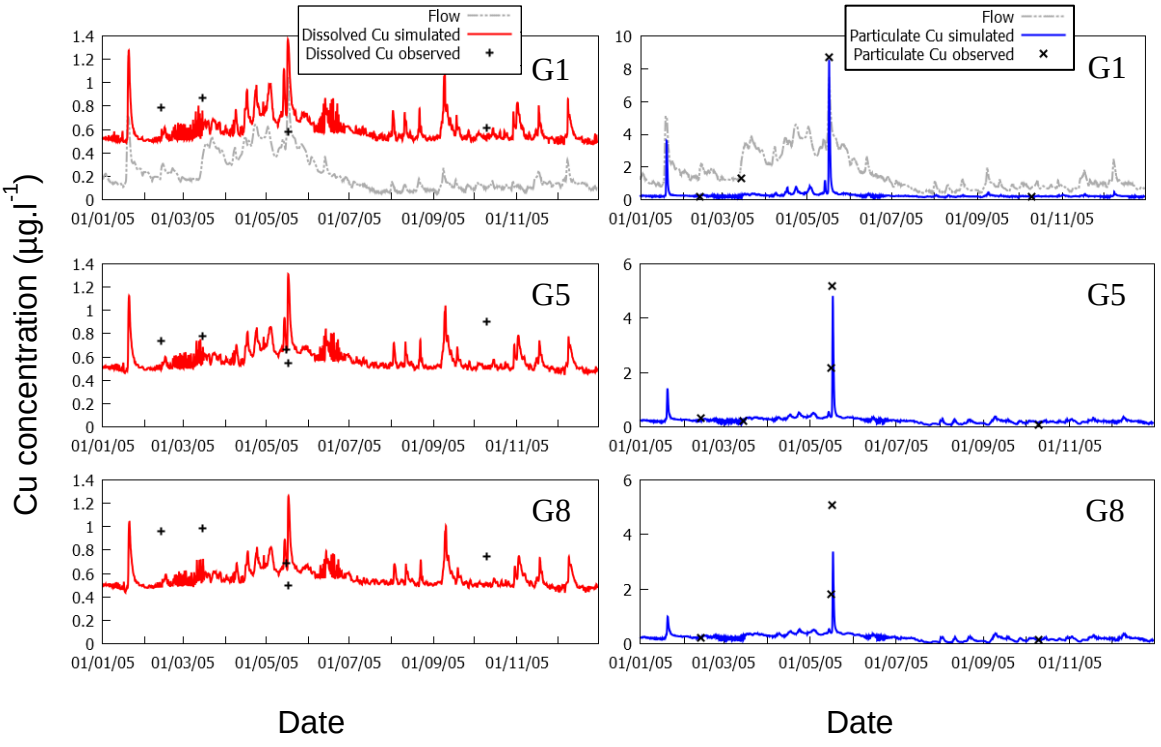

Figure 3: Annual Variation of simulated Cu concentration in the dissolved (left) and particulate (right) phases at three sampling points G1, G5 and G8 (top right corner, see Figure 1) during the year 2005. The observations (Aubert et al., unpublished data) collected during the four sampling campaigns are identified by crosses. The simulated flow at the first sampling point (G1) is shown to provide the hydrological context of the data.

Diurnal variations were predicted during two main periods: the winter low flow period (beginning of March) and the high flow recession in June. During these two periods, the concentrations of the dissolved and particulate fractions were of the same magnitude. Exchanges between the particulate and dissolved fractions of up to 30 % of Cu was predicted along the diurnal cycle. For the rest of the year, the dissolved Cu correlated with discharge while the particulate Cu correlated with the SPM concentration.

Overall, the simulated data are always in the range of the observations (Figure 3). Nevertheless, the high flow of May underestimated the concentration in the particulate phase at G5 and G8 while the dissolved phase was overestimated at the three sites.

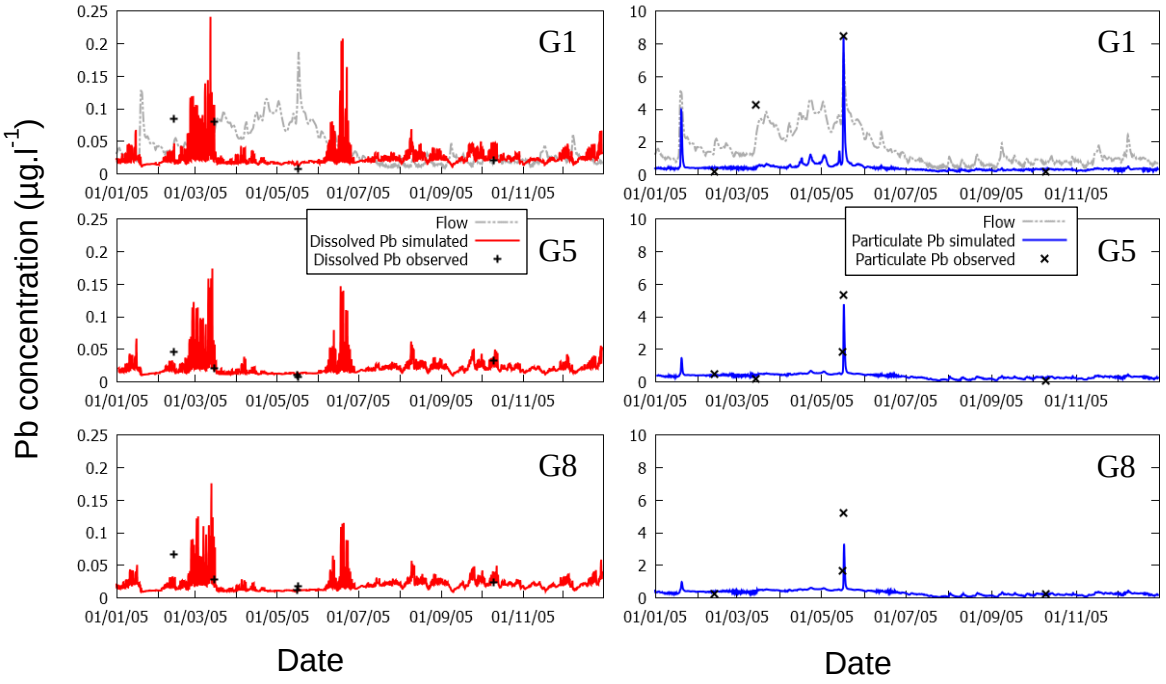

Figure 4: Annual Variation of simulated Pb concentration in the dissolved (left) and particulate (right) phase at the three sampling points G1, G5 and G8 (top right corner, see Figure 1) during the year 2005. The observations (Aubert et al., unpublished data) collected during the four sampling campaigns are identified by crosses. The simulated flow at the first sampling point (G1) is shown to provide the hydrological context of the data.

The concentrations of dissolved and particulate Pb differed by up to two orders of magnitude, the particulate fraction being dominant, especially during high flows. The high flows of January and May suggest important sedimentation rates since the simulated peak of concentrations drops from 9 $\mu g.l^{-1}$ to 4 $\mu g.l^{-1}$ from the sampling point G1 to the sampling point G8.

The two periods showing a diurnal pattern presented the same behaviour for Pb and Cu. During these periods, the daily pH variation induced an important variation in the partitioning of the TMs.

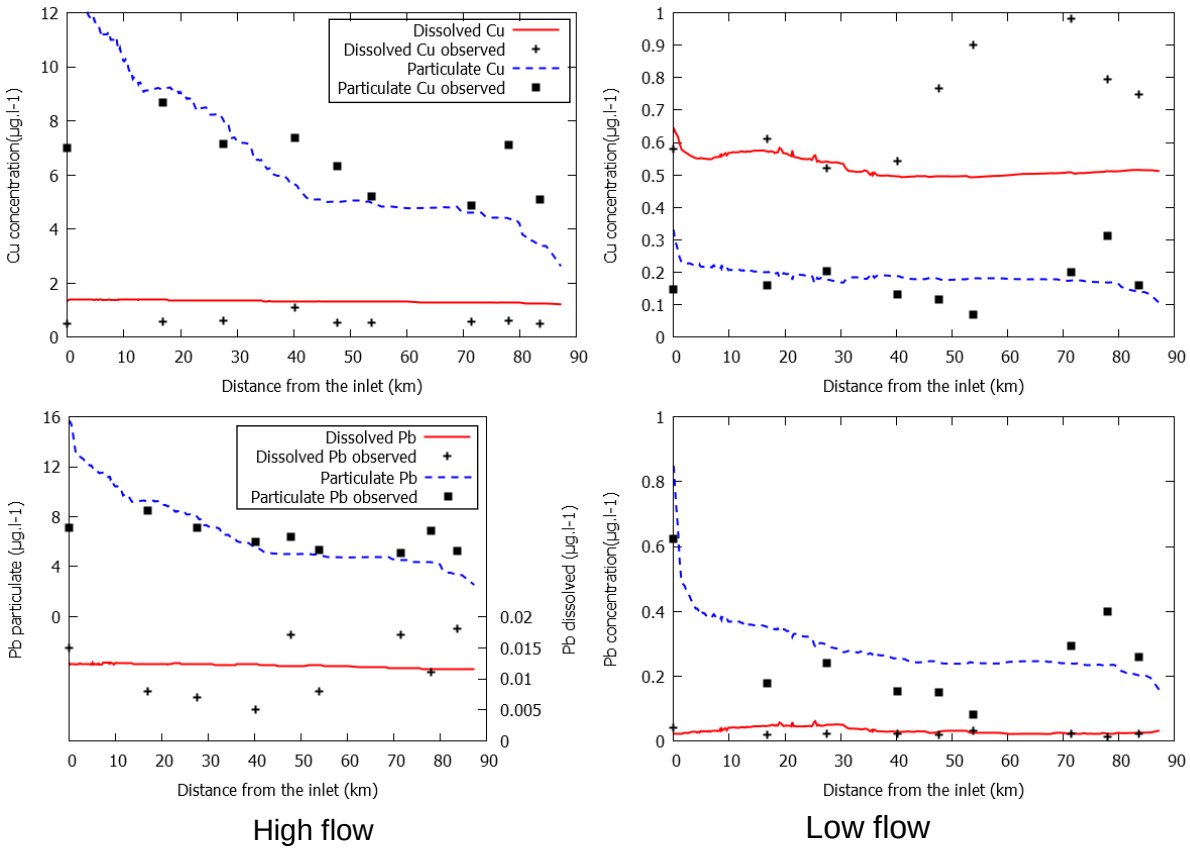

Figure 5: Profile of the TMs concentration along the river. The top figures refer to Cu while the bottom figures refer to Pb. The profiles at the left are the simulations and observations made during the high flow (800 $m^3.s^{-1}$) of 18 May 2005. The profiles at the right are the simulations (this study) and observations (Aubert et al., unpublished data) made during the low flow (80 $m^3.s^{-1}$) of 10 October 2005. The observations were made at Portet (at the inlet) and at the eight sampling stations (G1 to G8).

Figure 5 shows the longitudinal profile of the TMs during the two most contrasting conditions: the high flow of 18 May 2005 and the low flow period of 10 October 2005. The predicted profile of Cu under high flow conditions followed the trend of the observations. The dissolved fraction was slightly overestimated by the model, but it was of the same order of magnitude as the observations. The profile of Pb, in turn, suggested that most of the total concentration was transported by the particulate phase. In both cases, an obvious decrease in the concentration of the particulate fraction with distance from the upstream boundary was simulated.

The low flow profiles exhibited more spatial dynamics. Copper is carried mainly in the dissolved phase, leading to very little predicted variation in dissolved concentrations in the last 50km of the sector. Although they did not follow exactly the trend of the observations, the simulated concentrations were coherent with the observed concentrations. Part of the excess observed Cu comes from the tributaries. However, these tributaries did not contribute more than 10% of the total observed Cu flux. The profile of particulate Pb during low flow exhibits an important decrease in the first kilometers followed by smoother

dynamics. The dissolved Pb concentration is once again much lower than the particulate fraction, but is not negligible.

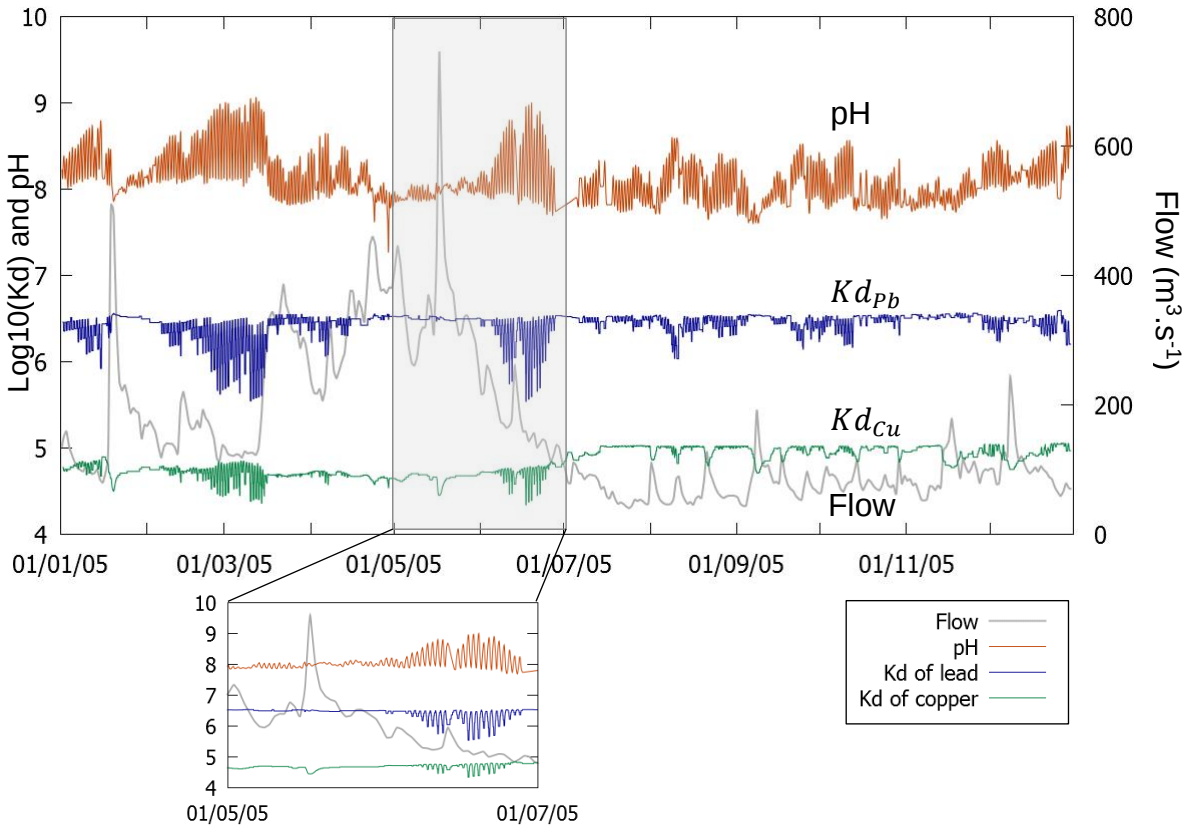

Figure 6: Variation of the simulated Kd of Cu (A) and Pb (B) under variable hydrological conditions during the year 2005. The Kd was calculated at the sampling point G5 (54 km after the inlet). The Kd is presented with the flow and the observed pH in the river. A zoom is provided over the high flow of May and the following diurnal cycles.

Figure 6 shows the variation of the simulated Kd under varying hydrological conditions for the two TMs. In both cases, the large diurnal variation in pH led to an important variation of the Kd particularly obvious in March and May 2005, whereas during the summer low flows, this diurnal variation led to limited Kd variation. For both Pb and Cu, the diurnal variations of pH and Kd presented an opposite relationship. Finally, high flow influenced the global physico-chemistry of the water by reducing the diel variation of the pH, and thus of the Kds. Under the considered hypothesis, the simulated Kd of Pb varied between 5.55 and 6.55 and the simulated Kd of Cu varied between 4.34 and 5.03.

3.3 Compared simulations of metal concentration in dissolved and particulate phases (Cu and Pb) using a fixed Kd model coupled to MOHID

The MOHID model was run with a fixed Kd (minimum and maximum values) to simulate the fate of Cu and Pb concentrations in the dissolved and particulate fractions for a given river station (G5, Figure 7).

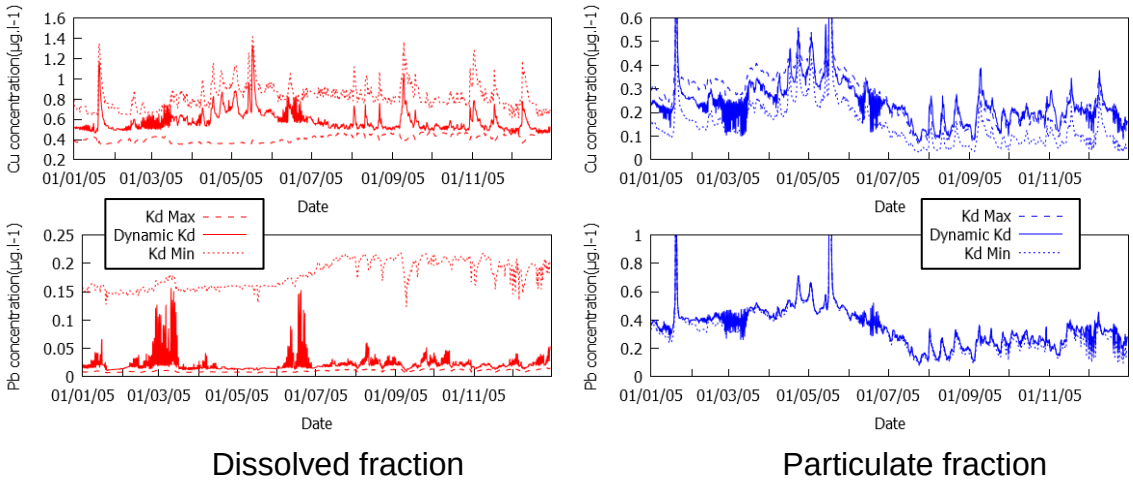

Figure 7: Comparison of dissolved (left) and particulate concentrations (right) for Cu (up) and Pb (down) at the sampling point G5 simulated by the dynamic MOHID – WHAM model with the constant Kd model of sorption. Two Kd have been used: the maximum and the minimum Kd observed during the sampling campaign (see Table 5). The figure does not show the maximal concentration of January and May high flows as all three scenarios presented a mismatch of less than 5% during these two events.

A variation of 0.58 units Kd of Cu led to major differences in predicted concentrations in both the dissolved and particulate fractions. For Pb, the pattern was different since a Kd variation of 1.25 units meant an increase of over 1000% in the dissolved fraction, while having limited impact on the particulate fraction. The dissolved TMs simulated by the MOHID – WHAM model are always between those predicted by the two fixed Kd scenarios, while the predicted particulate TMs oscillate above and below the fixed Kds.

3.4 Simulations of the accumulation of metal along the river continuum

The accumulated mass of TM per meter of river is presented in Figure 8 while the total accumulated mass of TM is presented in Table 8.

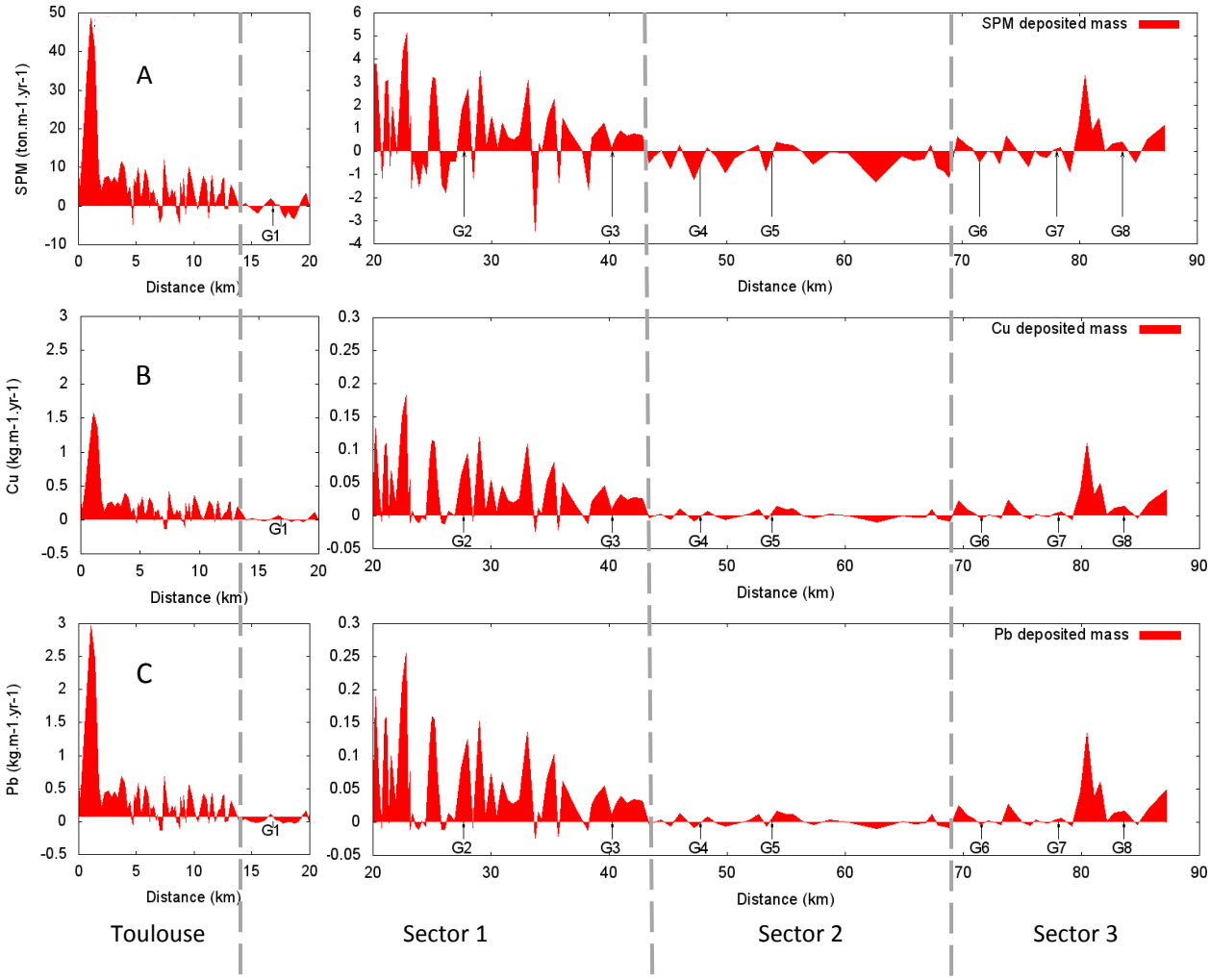

Figure 8: Accumulated (positive) or eroded (negative) mass of SPM (A), Cu (B) and Pb (C) along the river profile over the year 2005, according to the MOHID – WHAM model. The sampling points (from G1 to G8) are indicated. The river exits the city of Toulouse after 14 km where high sedimentation rates are simulated. Therefore, the scale is different before and after the city (left diagrams). The alluvial plain is further decomposed in three sectors exhibiting different behaviors (sectors 1 to 3).

The accumulated mass per meter of river allowed dividing the river in two sections: the passing of Toulouse city from the inlet of the river down to kilometer 14, and the alluvial plain from kilometer 14 down to the outlet of the modeled river sector (km 87). With its numerous bridges and three dams, the city of Toulouse showed high accumulation zones compared to the rest of the studied sector. The alluvial plain could be divided into three additional sectors. Sector 1 corresponded to kilometers 14 to 45, where high deposition rates occurred. Sector 2 was from kilometers 43 to 70, where the erosion processes and sedimentation were in balance, and sector 3 was from kilometer 70 to the outlet of the alluvial plain (km 87) and the start of the influence of the Malause reservoir. The accumulation of Cu followed the same pattern as the accumulation of Pb, but the absolute fluxes were much lower in the passing of Toulouse city.

Table 8: Annual fluxes of SPM, Cu and Pb entering the river upstream of Toulouse and annual accumulated mass of each TM according to the three scenarios (MOHID – WHAM scenario, fixed Kd to the minimum observed value and to the maximum observed value). The SPM model was the same one for the three scenarios. The ratio of the accumulated mass divided by the annual flux is given within parentheses.

	Annual flux ($kg.yr^{-1}$)	Total accumulated ($kg.yr^{-1}$) (% of the annual flux)		
		MOHID – WHAM	Kd Min	Kd Max
SPM	1.61E+8	1.10E+8 (68%)		
Cu	9230	4563 (49%)	3819 (41%)	5635 (61%)
Pb	9779	7633 (78%)	6998 (71%)	7679 (79%)

Similar annual fluxes of Pb and Cu were provided as input to the model. However, the mass of TM that accumulated on the riverbed depended on the scenario. The scenario of the MOHID – WHAM model suggested that 49% of Cu and 78% of Pb that enters the river would deposit within the river sector. In the case of Cu, the accumulation corresponded roughly to the average of the two others scenarios (fixed Kd to a minimum and a maximum value), while the case of Pb suggested that the total accumulated fluxes were similar for the three scenarios.

3.5 Sensitivity analysis

The result of the sensitivity analysis is presented for the two TM and the two scores in Table 9.

Table 9: Results of sensitivity analysis. Each parameter is ranked from 1 (most influential) to 34 (least influential) for the average Kd and the dispersion of the Kd. The rank indicated is the highest rank achieved by the parameter over the whole study site, which explains that some ranks are missing. The very influential parameters (dark grey) and the influential parameters (light grey) are highlighted.

		Average Kd		Kd dispersion		
Factor	No.	Cu	Pb	Cu	Pb	Global rank
pH	32	1	1	1	1	1
Manning	1	4	6	1	1	1
$\tau_{ero\,2}$	10	7	8	1	3	1
E_2	11	4	6	1	2	1
$W_{C\,2}$	12	12	9	1	1	1
$\tau_{sed\,2}$	13	12	12	4	1	1
$W_{C\,1}$	8	7	10	2	3	2
f_{FeOH}	15	3	2	7	9	2
f_{res}	22	2	3	19	13	2
POC_{NUM}	16	3	22	6	16	3
$\tau_{sed\,1}$	9	17	13	11	4	4
PCO_2	33	6	4	18	16	4
TM_{sed}	5	14	7	13	5	5
[Fe]	28	9	5	15	14	5
E_1	7	14	15	10	7	7
Diffusivity	2	22	24	8	12	8
$\tau_{ero\,1}$	6	15	17	8	8	8
[Al]	25	21	9	20	19	9
[DOC]	21	10	13	23	22	10
[Mg]	24	20	10	19	18	10
SPM_{MIN}	17	17	26	13	20	13
$[SO_4]$	31	23	14	24	23	14
[Ca]	27	15	16	16	15	15
F_{HA}	14	22	24	17	21	17
[Cl]	29	26	20	26	25	20
[Na]	23	24	21	25	27	21
$[NO_3]$	30	27	25	27	27	25
α	3	30	29	29	26	26
f_{clay}	19	28	29	27	29	27
[K]	26	28	28	29	30	28
A_S	4	30	29	29	29	29
$f_{POC_{MIN}}$	18	31	29	33	30	29
f_{MnOH}	20	29	29	29	33	29
ΔT	34	30	29	33	33	29

The MOHID – WHAM coupled model is very sensitive to the pH. This parameter is very influential for both TMs and under the two scores considered. The pH was the only very influential parameter for the average Kd. The dispersion of the Kd, i.e. its variation under contrasted hydrodynamic and physico-chemical conditions, was also very sensitive to the Manning coefficient and the four erosion – sedimentation parameters related to the class 1 SPM (coarser SPM than the class 2). The average Kd was sensitive to six parameters, among which one was related to hydrodynamics (the Manning coefficient), one to erosion – sedimentation (E_2) and four to the chemistry ($f_{FeOH}, f_{res}, POC_{NUM}, PCO_2$). The dispersion of Kd was sensitive to two additional parameters linked to erosion – sedimentation rates ($W_{C\,1}, \tau_{sed\,1}$).

4 Discussion

4.1 Hydrodynamic model

The use of 1D hydraulic equations means that the water is fully homogenous within a finite volume element, has no lateral velocity and thus cannot represent the influence of the meanders. Furthermore, there is no coupling between the river and the groundwater apart from the conceptual transient storage zone of the OTIS equations. Nevertheless, the use of St-Venant equations allows computation of variable flow velocity and thus, variable shear stress with respect to the local slope of the river. In turn, this shear stress, computed with the help of hydraulic variables, drives the full erosion – sedimentation equations, which account for the SPM concentration along the river. Therefore, the most important process affecting the transport of TMs is definitely the hydraulic description of the river.

The transient storage model OTIS allows differentiation of the flow velocity and the transport velocity of suspended elements, the latter being slower (Bencala and Walters, 1983). It was also successfully applied to tracer experiments simulating pollutant spill (Bencala and Walters, 1983; Garneau et al., 2015; Runkel et al., 1999), but in absence of major disturbances (such as a tracer test or spill) or in long term simulation (larger than the residence time of the water in the river), its influence was found to be negligible with respect to the other processes.

The erosion – sedimentation model based on the Partheniades (1965) equations allows the fine morphology of the river to be taken into account. The SWAT model also proposes erosion – sedimentation equations and suggests separating the sediment into four size classes (gravel, sand, silt and clay). But the alluvial plain of the Garonne River is known to transport fine sediments related to fine sand, silt and clays (Garneau et al., 2015; Steiger and Gurnell, 2003), thus allowing to neglect the transport of coarse sand and gravel. Furthermore, as the SPM characteristics depend on the hydrology, it was necessary to describe their behavior with more than one class. Using two classes is common (El Ganaoui et al., 2004; Ziervogel and Bohling, 2003) and provided acceptable results for modelling the transport of particulate TMs. Indeed, erosion – sedimentation processes could be better modelled by using grain size distribution of the sediment. But only approximated and measured data were available from Steiger and Gurnell (2003) and

Steiger et al. (2001b) during specific floods, respectively. It was thus considered that before integrating fine grain size distribution to the model, additional measures would be required under various hydrological conditions.

4.2 Assessment of the modelling hypotheses

The coupled model MOHID – WHAM is driven by strong hypotheses. The most important in the scope of TM modelling is the actual TM concentration provided as input. In a complex watershed such as the Garonne one, the sources of TMs depend on the source of the water. Semhi (1996) and Semhi et al. (2000a, 2000b), for example, demonstrated that the chemical properties of the water coming from the different tributaries of the Garonne varied according to the geological composition of the sub-watersheds. The flow path of the water from rainfall to river also alters its chemical composition, as shown from stable isotopic studies (Siegel, 1983). Mixing between groundwater and runoff contributions to the river can be achieved by distributed hydrological modelling but was beyond the scope of this work. Therefore, estimating the initial water composition at the inlet of the study case is far from trivial. The hypotheses used were driven by field data and allowed good estimation of the TM concentrations under most hydrological conditions. The concentrations of major ions were fixed to constant values throughout the year. Such an assumption has previously been used by Farley et al (2011) for similar modelling of trace metals in lakes. The carbonates, which are the main buffer in the Garonne River, show important concentrations (from 1 to 5 $mmol.l^{-1}$) (Probst and Bazerbachi, 1986; Semhi, 1996), but since their temporal variability is unknown, a fixed concentration was used. Similar considerations apply to the DOC concentration, which is likely to be important in controlling Kds for both TMs, but particularly Cu.

The variation in pH was recorded at the upstream boundary of the study sector. Its variation between 7.2 and 9.2 is characteristic of a well buffered river, as already identified in many studies (Etchanchu and Probst, 1988; Probst, 1983; Probst and Bazerbachi, 1986; Semhi et al., 2000a, 2000b). A diel variation over more than one unit is characteristic of biological photosynthesis and respiration (Nimick et al., 2011; Wright and Mills, 1967) and according to Nimick et al. (2011), diel variations at pH between 8.0 and 9.0 exhibit the largest pH amplitude between day and night, most likely due to a $CaCO_{3(s)}$ – $CO_{2(g)}$ buffering. During high flows, this diel variation is reduced by increased turbidity and the detachment of biofilm, which reduces photosynthesis (Boulêtreau et al., 2006; Uehlinger et al., 1996).

The POC concentration estimation was an important parameter to consider because many TMs are known to bind preferentially with organic material, and because the organic content is known to vary greatly with the hydrological conditions. The relationship between the fraction of POC and the SPM concentration is well known and has been observed in many rivers around the world (Ludwig et al., 1996; Meybeck, 1982). Therefore, the equation provided in Table 3 can be applied to most rivers, although the parameters should be recalibrated with respect to the river's watershed and dynamics (Boithias et al., 2014). The separation of the POC into humic and fulvic acids can be done with many different approaches. The approximation of a 50%-50% separation of the POC in humic and fulvic acids is suggested as the POC composition is

usually unknown, although some studies did calibrate the concentration of “active” humic substances to optimise model performance (Dwane and Tipping, 1998; Tipping et al., 2003). In this work, though, the scarcity of data prevented the use of a calibration – validation procedure. Therefore, the default 50%-50% separation was used.

At the operating pH, the manganese oxide and the clays were predicted by WHAM to play marginal roles in the transport of TMs. Therefore, their fractions could be fixed to their average concentration without significant impact on the global transport. The iron oxides, on the other hand, have been shown to be highly correlated to particulate Pb (Bur et al., 2009; Lofts and Tipping, 2000). It was deemed reasonable to fix the iron oxide at the average concentration of iron, but providing a finer description of these oxides certainly would improve the fit between observations and simulation. Such finer description could include the colloidal iron oxides in the dissolved phase, as suggested by Lofts and Tipping (2000).

4.3 Application of the coupled model to the study case

Although some modelling studies have simulated TM transport for a specific hydrological event or over a few days (Ji et al., 2002; Lindenschmidt et al., 2006), these simulations represent the first attempt to simulate the fate of TMs under contrasting hydrology and morphology, based on physical and chemical models, in a large river.

The hydraulic model was constructed with the help of a simplified description of the morphology by including more than 200 profiles of the riverbed over the 87 km of the sector. However, the spacing between every profile ranged from 40 meters to 2.3 km. The scarce profile density in sector 3 can be seen on Figure 8. Therefore, some meanders and riffle – pool successions could not be accurately described in this section (Steiger et al., 2001a). Since these hydraulic units are known to be an important sink for some nutrients (Bonvallet Garay et al., 2001) or to generate important water exchanges between the river and the groundwater (Peyrard et al., 2008), important attention should be given to a fine description of the riverbed through its cross-section profiles.

The OTIS model proved to add negligible information on the Garonne River. This effect is explained by the relatively short time influence of the transient storage with respect to the simulation time. It is likely that in some contexts, simulation of transient storage will allow for robust modelling at finer temporal and spatial scales. But in the actual context, it was not possible to detect its effect on the transport of TMs.

The SPM model is critical for a proper description of the TMs bound to the particulate phase. The parameterization of the SPM model provided optimal parameter sets similar to those presented in Garneau et al. (2015). The use of turbidity measurements to estimate the SPM concentration as input provided a consistent detailed input to the model. However, the contribution from the tributaries was neglected since they account for less than 2% of the flow and no SPM concentration data was available. However these contributions can, in the case of localised high flows, be important (Oeurng et al., 2010). The detachment of epilithic biofilm is another known source of SPM which was not taken into account

(Boulêtreau et al., 2006). These two processes are a possible explanation for the difference between the modelled and observed SPM. Nevertheless, the SPM model provided a consistent representation of the SPM observations in various points of the river and was deemed sufficient for the TM modelling.

The simulation of Cu and Pb and their dissolved and particulate fractions in the Garonne River shows that the input assumptions and the model are capable of representing the magnitude of the observations. Two main processes affect the concentrations and the different fractions of Pb and Cu: the hydrological conditions and the diurnal variation in the pH. The hydrological conditions were responsible for the highest concentrations of Cu (dissolved and particulate) and for particulate Pb. The dissolved Pb was much more affected by the pH variation, with concentrations varying by up to 1000%. Because of its higher concentrations, the particulate fraction of Pb varied by less than 30% during the diurnal cycles. According to WHAM, carbonate complex formation with Pb and Cu is predicted to reduce Kds when the pH goes up to 9.0. This effect is in opposition to diurnal cycles usually observed (Nimick et al., 2011) and TMs and additional observations should be sought on the study case to confirm this simulation result. However, contrary of the works of Nimick et al. (2011), the Garonne River does not experience important metal contamination.

The variation of the Kd through the year is explained by two processes: the variation of POC concentrations with respect to the SPM concentrations, and the daily variation of the pH. The first process is highlighted in the case of Cu during the high flow period of May 2005, where the SPM concentrations are high and the daily variation of the pH is low, and during the summer low flows (August to October) where the SPM concentrations are minimal. These low SPM concentrations lead to a maximal POC fraction of 24% (see Table 3) and the Kd was controlled by the ratio $(\%POC\ in\ SPM)/DOC$ since Cu binds mostly on the organic carbon (Dwane and Tipping, 1998). The model WHAM predicts, however, that Pb binds mostly to iron and manganese oxides. Therefore, the POC influence was not visible on the Kd of Pb. Winter low flow conditions differ from the summer ones. The river flow and biomass production are higher (Boulêtreau et al., 2006). Under these conditions, the proposed model suggests a much larger diurnal variation in Kd due to the diel variation of the pH and larger SPM concentrations. These results suggest an important variation in the sub-daily concentration of the dissolved and particulate phases that have been observed in some studies (Brick and Moore, 1996; Kimball and Runkel, 2009; Nimick et al., 2011, 2003; Tercier-Waeber et al., 2009). Brick and Moore (1996) reported increases in dissolved TMs concentrations (two to three times higher than daytime concentrations) at night in waters with similar pH and major ion concentrations, showing high concentrations of TMs. However, the modelling assumptions must be borne in mind, because the CO_2 partial pressure, the concentrations of major ions and DOC, and the concentrations of metal oxides per unit mass of SPM were kept constant throughout the simulation. These assumptions led the WHAM model to predict desorption of both Cu and Pb as pH increased, as the formation of carbonate complexes increased. This effect is opposite to that seen by Brick and Moore (1996), however Tercier-Waeber et al. (2009) emphasized the importance of the complex chemistry of

natural waters for explaining irregular diurnal cycles of dissolved trace metal concentration (Pb, Cu and Cd). Nevertheless, since the sub-daily behaviour of metals and trace metals was not characterized in the Garonne River, the simulation remains the best approximation available.

The “particle concentration effect”, described in numerous studies (Di Toro et al., 1986; Guéguen and Dominik, 2003; Honeyman and Santschi, 1988), is the reduced capacity of SPM to bind to TMs as the concentration of SPM rises. The coupled model used represents this particle effect by the separation of the SPM into different fractions with different POC contents. It is also possible to adjust the colloidal concentrations of DOC, metal oxides and major ions, as proposed by Tipping et al. (1998). The perturbation of the Kd by the SPM characterization can be observed in the case of Cu during the high flow. Since Cu binds mostly to organic matter, an increase in SPM results in a decrease of the POC fraction in the SPM and a decrease in the Kd. The simulated Pb does not exhibit a particle effect, but once again, this can be related to the modelling hypotheses. Since Pb mostly binds on iron and manganese oxides and since their concentrations and the concentrations of competing major ions are kept constant, the equilibrium of dissolved and particulate Pb is not affected through the simulation.

4.4 Comparison between the dynamic Kd and the fixed Kd simulation

The comparison of the fixed Kd simulation to the dynamic Kd (see Figure 7) allows assessment of the importance of the chemical model. The dynamic Kd predicts a very dynamic behaviour of the dissolved phase for both TMs while the particulate phase is much more stable. The dynamic Kd scenario also allows the importance of the hydrology to be highlighted. In the case of Cu, the fixed Kd scenarios suggested that the concentration in the dissolved phase remained more or less constant, with a noticeable dilution during the high flow. The dynamic Kd scenario rather suggested that the dissolved Cu would progressively move from the maximal Kd scenario to the minimal Kd scenario over a two months’ period. Since that period includes the highest fluxes of Cu (important flows and SPM concentrations), the dynamics of the Kd plays an important role in the predicted total mass balance of TMs.

The main advantage of a fixed Kd model is its simplicity but this simplicity forces the modeller to stick to very stable conditions or very short (with respect to hydrology) time windows. Ji et al. (2002) modelled the behaviour of TMs over high flow using a fixed Kd. However, as shown on Figure 7, the fixed Kd model is not robust, as it cannot reliably be used to forecast TMs in conditions different from those used for its calibration.

The definition of the ratio of the particulate – dissolved fraction is also of prime importance. For example, Johansson et al. (2001) suggest using the particulate fraction (PF), i.e. the ratio of the particulate to the total concentration of TM with all concentrations in $kg.l^{-1}$ instead of the Kd. If this choice can be justified in lakes where the SPM concentrations are low and do not vary significantly, SPM concentrations in rivers can increase by several orders of magnitude according to the hydrological conditions. The PF in these

conditions would simulate a dissolved concentration of TM linearly dependent on the particulate concentration which, according to Figure 3 and Figure 4, is definitely not the case.

The choice of a fixed or variable Kd can therefore determine which control parameters will be highlighted. If the objective of a study is to assess the mass-balance of a TM over a river, a careful choice of fixed Kd will return a good approximation of reality, especially for highly particulate TMs such as Pb. In the other hand, if a finer description of TM dynamics is desired, processes such as diurnal pH variation proved to be of great importance in some hydrological conditions and the variation of the Kd significantly altered the concentration of both the dissolved and particulate fractions of TMs.

Furthermore, many studies required to know the colloidal fraction of TMs (Guéguen and Dominik, 2003; Kimball and Runkel, 2009; Nimick et al., 2003). Although this separation does not affect the path of TMs since they are considered to stay in the water column, the WHAM model computes these fractions natively by calculating the full speciation of the TMs and by explicitly considering the colloidal concentrations of organic matter and metal oxides. This information has been used in various water quality and ecotoxicology studies with success (Balistrieri and Mebane, 2014; Farley et al., 2011; Gandois et al., 2010).

4.5 Spatial accumulation of TM and influence of the hydromorphology

Modelling the spatial accumulation of TM allows quantification of the importance of different zones along the river. Figure 8 suggests that the segment of the river passing through the city of Toulouse acts as the most important sink for TMs. These sedimentation zones are due to multiple weir which generates deep water (S.M.E.P.A.G., 1989). Predicted sediment accumulation compares favourably with previous estimates of accumulation (Steiger et al., 2001a; Steiger and Gurnell, 2003) that reached up to 160 $kg.m^{-2}$ of sediment in the alluvial plain of the Garonne River during the flood of October 1992 (Q_{max} of 2620 $m^3.s^{-1}$). Considering an average riverbed width of 75 meters between Portet and Toulouse (the region which exhibits the largest sedimentation rates), such a flood would lead to an accumulation of sediment up to 12 $ton.m^{-1}$. This figure is higher than the modelled accumulation (up to 5 $ton.m^{-1}$), but the floods studied by Steiger and Gurnell (2003) were significantly larger than the highest flow simulated in these works (Q_{max} of 800 $m^3.s^{-1}$ in May 2005).

After the high sedimentation zone at the passage of Toulouse city, the spatial accumulation profile of TMs depends on the fine and very fine SPM present. The fine SPM is mostly imported from upstream since it requires high shear stress to be eroded and the tributaries of the sector are neglected in the model. Therefore, a deposition of fine SPM and associated TMs is observed in sector 1 (Figure 8). Furthermore, the second sector of the alluvial plain exhibits higher flow velocity, thus inhibiting loss of the remaining fine SPM without generating sufficient shear stress to erode new material. The remaining fine SPM finally settles in the third sector, where the influence of the Malause reservoir begins. The very fine SPM settles

only in the deepest pools and is the main source of eroded material along the sector. The influence of the riffle and pools (sector 1) after Toulouse is thus clearly visible, with its fast succession of erosion and sedimentation zones. The second sector is a net source of very fine SPM, with an average shear stress generating erosion along the whole sector. The riffle and pool succession could not be identified from the riverbed profile due to a limited number of available profiles. Finally, the third sector meets the conditions for a high sedimentation of the very fine SPM and associated TMs. The model is therefore capable of predicting both the accumulation and the erosion of TMs in the sediment.

4.6 Most influential parameters in the sensitivity analysis

The influence of pH on Kd is well known (Drever, 1997). It was therefore predictable that the sensitivity analysis would identify pH as a very influential parameter for both TMs and both scores. The sensitivity analysis also highlighted the influence of the erosion – sedimentation process on the dispersion of the Kd. This influence is due to the SPM composition which changes with its concentration in water, according to the modeling hypotheses used and to previous measurements (Probst, 1992; Probst and Bazerbachi, 1986). It also shows that a proper modeling of the SPM composition is fundamental to simulate the Kd under contrasting hydrodynamic conditions. Finally, it must be noted that the average Kd of the two TMs used was sensitive to different factors. The average Kd of Cu was sensitive to the organic carbon, which is related to the parameter POC_{NUM} while the average Kd of Pb was sensitive to the carbonates chemistry, related to the PCO_2 parameter. These results are consistent with previous sensitivity analysis performed on WHAM. For example, Cory et al. (2007) showed that aluminium speciation was very sensitive to pH and DOC, along with other major ions (Fe, Ca and Mg). Cloutier-Hurteau et al. (2007) further suggested that Cu was most sensitive to DOC and that its calibration was necessary to provide good speciation results of Cu. In the present study, the organic carbon was also an influential parameter, with the presence of the POC_{NUM} parameter among the influential parameters.

The Morris sensitivity analysis cannot quantify non-linear effects or correlation between parameters and has many detractors (Saltelli and Annoni, 2010). However, its efficiency as a cheap exploratory sensitivity analysis has been demonstrated in a large number of applications (Campolongo and Saltelli, 1997). Therefore, a robust initial ranking of the parameters can be achieved.

5 Conclusion and outcomes

The coupled model MOHID – WHAM has been developed as a mechanistic model capable of simulating the hydrodynamics of a large river, and the behaviour of SPM and TMs associated with the transport of the inner material in the river channel, according to the water chemical composition.

The model showed its ability to be applied to a large, morphologically complex river under contrasting hydrological conditions, improving the understanding of TM dynamics and highlighting key controlling

parameters. The dynamic of a TM such as Cu, which undergoes complex sorption – desorption, was highly influenced by the dynamic variation of the partition coefficient between particulate and dissolved fractions. The dynamic of Pb, in turn, was much more influenced by the particulate fraction. But the dissolved fraction showed large variations when diurnal cycles of the pH were stronger, highlighting the most probable importance of sub-daily processes in altering significantly the state of the TMs in the rivers. The model could thus suggest new sampling strategies based on the diurnal cycles particularly to assess the implication of TMs contamination in ecotoxicology.

The MOHID – fixed Kd scenario also suggested that between 41 and 61% of Cu and 71 to 79% of Pb entering the river would sediment in the riverbed before reaching the outlet of the modelled sector. The MOHID – WHAM model refined these estimates to 49% for Cu and 78% for Pb.

The description of the complex hydromorphology allowed identification of zones of significant sedimentation *vs* erosion, thus allowing assessment of the potential contamination of the sediment. The case of lead showed that the large diurnal variation did not generate large variation in total fluxes to the sediment. For copper, it was shown that using a dynamic Kd led to a very different accumulation pattern compared to the fixed Kd alternatives, highlighting the importance of a proper description of the water chemistry. Furthermore, the dynamic Kd model can provide additional information such as the possibility to predict the free metal ion concentration, which is of importance for modelling metal bioavailability and toxicity.

Being a physically and chemically mechanistic model, the coupled MOHID – WHAM model requires extensive databases and a large number of parameters. But by focusing on the influential variables, such as pH, SPM, POC and pCO_2, new conceptual models to estimate the Kd of TMs could be developed. The model presented here and applied to Cu and Pb cannot be generalized to other TMs without performing additional computations. Nevertheless, the path for fast, versatile and precise Kd computation is open. In its current form, the MOHID – WHAM coupled model offers numerous potential applications, from mass-balance of TMs to pollution transfer scenarios.

6 Acknowledgements

These works were funded by the French Ministry for Higher Education and Research and the project ANR ADAPTEAU / ANR-11-CEPL-008. Travel expenses for CEH stay (UK) were funded by the Paul Sabatier University through the ATUPS program. Most of the data were collected in the scope of the project P2 GIS Ecobag, which participants are warmly thanked, and particularly Dominique Aubert for trace metals data attainments. Laure Gandois is thanked for discussion on the performance of WHAM in the initial stages of the study and Jean-Luc Probst for discussions on the Garonne river chemical status, particularly for carbon and suspended matter modelling.

7 References

Allen, P.M., Arnold, J., Jakubowski, E., 1999. Prediction of stream channel erosion potential. Environ. Eng. Geosci. 5, 339–351.

Allison, J.D., Allison, T.D., 2005. Partition coefficients for metals in surface water, soil, and waste (No. EPA/600/R-05/074). U.S. Environmental Protection Agency, Athens, GA, US.

Allison, J.D., Brown, D.S., Novo-Gradac, K.J., 1991. MINTEQA2/PRODEFA2, A Geochemical Assessment Model for Environmental Systems: Version 3.0 User's Manual.

Almås, Å.R., Lofts, S., Mulder, J., Tipping, E., 2007. Solubility of major cations and Cu, Zn and Cd in soil extracts of some contaminated agricultural soils near a zinc smelter in Norway: modelling with a multisurface extension of WHAM. Eur. J. Soil Sci. 58, 1074–1086. doi:10.1111/j.1365-2389.2007.00894.x

Ambrose, R.B., Wool, T.A., Martin, J.L., 1993. The Water Quality Simulation Program, WASP5: Model Theory, User's Manual and Programmer's Guide. U.S. Environmental Protection Agency, Athens, GA, US.

Aubert, D., Probst, J.-L., Probst, A., submitted. Influence of hydrological conditions on trace metal behaviour and dissolved/particulate partitioning in the upper Garonne and Ariège rivers (SW, France). J. Hydrol.

Audry, S., Schäfer, J., Blanc, G., Bossy, C., Lavaux, G., 2004. Anthropogenic components of heavy metal (Cd, Zn, Cu, Pb) budgets in the Lot-Garonne fluvial system (France). Appl. Geochem. 19, 769–786. doi:10.1016/j.apgeochem.2003.10.002

Balistrieri, L.S., Mebane, C.A., 2014. Predicting the toxicity of metal mixtures. Sci. Total Environ. 466–467, 788–799. doi:10.1016/j.scitotenv.2013.07.034

Bencala, K.E., Walters, R.A., 1983. Simulation of solute transport in a mountain pool-and-riffle stream: A transient storage model. Water Resour. Res. 19, 718. doi:10.1029/WR019i003p00718

Bianchi, T.S., Wysocki, L.A., Stewart, M., Filley, T.R., McKee, B.A., 2007. Temporal variability in terrestrially-derived sources of particulate organic carbon in the lower Mississippi River and its upper tributaries. Geochim. Cosmochim. Acta 71, 4425–4437. doi:10.1016/j.gca.2007.07.011

Boithias, L., Sauvage, S., Merlina, G., Jean, S., Probst, J.-L., Sánchez Pérez, J.M., 2014. New insight into pesticide partition coefficient Kd for modelling pesticide fluvial transport: Application to an agricultural catchment in south-western France. Chemosphere 99, 134–142. doi:10.1016/j.chemosphere.2013.10.050

Bonvallet Garay, S., Sauvage, S., Vervier, P., 2001. Hydromorphological control of phosphorus in a large free-flowing gravel bed river: the Garonne River (France). Regul. Rivers Res. Manag. 17, 461–472. doi:10.1002/rrr.662

Bottacin-Busolin, A., Marion, A., Musner, T., Tregnaghi, M., Zaramella, M., 2011. Evidence of distinct contaminant transport patterns in rivers using tracer tests and a multiple domain retention model. Adv. Water Resour. 34, 737–746. doi:10.1016/j.advwatres.2011.03.005

Boulêtreau, S., Garabetian, F., Sauvage, S., Sánchez Pérez, J.-M., 2006. Assessing the importance of a self-generated detachment process in river biofilm models. Freshw. Biol. 51, 901–912. doi:10.1111/j.1365-2427.2006.01541.x

Brick, C.M., Moore, J.N., 1996. Diel variation of trace metals in the Upper Clark Fork river, Montana. Environ. Sci. Technol. 30, 1953–1960. doi:10.1021/es9506465

Brunel, C., Munoz, M., Probst, A., 2003. Remobilisation of Zn and Pb in a mountain stream contaminated by mining wastes during a moderate flood event (Ariège, France). J. Phys. IV Proc. 107, 233–236. doi:10.1051/jp4:20030285

Bryan, S.E., Tipping, E., Hamilton-Taylor, J., 2002. Comparison of measured and modelled copper binding by natural organic matter in freshwaters. Comp. Biochem. Physiol. Part C Toxicol. Pharmacol. 133, 37–49. doi:10.1016/S1532-0456(02)00083-2

Bur, T., Probst, J.L., N'guessan, M., Probst, A., 2009. Distribution and origin of lead in stream sediments from small agricultural catchments draining Miocene molassic deposits (SW France). Appl. Geochem. 24, 1324–1338. doi:10.1016/j.apgeochem.2009.04.004

Campolongo, F., Saltelli, A., 1997. Sensitivity analysis of an environmental model: an application of different analysis methods. Reliab. Eng. Syst. Saf., The Role of Sensitivity Analysis in the Corroboration of Models and its Links to Model Structural and Parametric Uncertainty 57, 49–69. doi:10.1016/S0951-8320(97)00021-5

Cao, J., Xue, H., Sigg, L., 2006. Effects of pH and Ca competition on complexation of cadmium by fulvic acids and by natural organic ligands from a river and a lake. Aquat. Geochem. 12, 375–387. doi:10.1007/s10498-006-9004-6

Caruso, B.S., 2004. Modeling metals transport and sediment/water interactions in a mining impacted mountain stream. JAWRA J. Am. Water Resour. Assoc. 40, 1603–1615. doi:10.1111/j.1752-1688.2004.tb01609.x

Caruso, B.S., Cox, T.J., Runkel, R.L., Velleux, M.L., Bencala, K.E., Nordstrom, D.K., Julien, P.Y., Butler, B.A., Alpers, C.N., Marion, A., Smith, K.S., 2008. Metals fate and transport modelling in streams and watersheds: state of the science and USEPA workshop review. Hydrol. Process. 22, 4011–4021. doi:10.1002/hyp.7114

Chapman, B.., Jones, D.., Jung, R.., 1983. Processes controlling metal ion attenuation in acid mine drainage streams. Geochim. Cosmochim. Acta 47, 1957–1973. doi:10.1016/0016-7037(83)90213-2

Christensen, J.B., Christensen, T.H., 2000. The effect of pH on the complexation of Cd, Ni and Zn by dissolved organic carbon from leachate-polluted groundwater. Water Res. 34, 3743–3754. doi:10.1016/S0043-1354(00)00127-5

Cloutier-Hurteau, B., Sauvé, S., Courchesne, F., 2007. Comparing WHAM 6 and MINEQL+ 4.5 for the Chemical Speciation of Cu2+ in the Rhizosphere of Forest Soils. Environ. Sci. Technol. 41, 8104–8110. doi:10.1021/es0708464

Cory, N., Andrén, C.M., Bishop, K., 2007. Modelling inorganic aluminium with WHAM in environmental monitoring. Appl. Geochem., Selected Papers from the 7th International Conference on Acid Deposition, Prague, Czech Republic, 12–17 June, 20057th International Conference on Acid Deposition 22, 1196–1201. doi:10.1016/j.apgeochem.2007.03.011

Dai, M.-H., Martin, J.-M., 1995. First data on trace metal level and behaviour in two major Arctic river-estuarine systems (Ob and Yenisey) and in the adjacent Kara Sea, Russia. Earth Planet. Sci. Lett. 131, 127–141. doi:10.1016/0012-821X(95)00021-4

Davide, V., Pardos, M., Diserens, J., Ugazio, G., Thomas, R., Dominik, J., 2003. Characterisation of bed sediments and suspension of the river Po (Italy) during normal and high flow conditions. Water Res. 37, 2847–2864. doi:10.1016/S0043-1354(03)00133-7

Di Toro, D.M., Allen, H.E., Bergman, H.L., Meyer, J.S., Paquin, P.R., Santore, R.C., 2001. Biotic ligand model of the acute toxicity of metals. 1. Technical Basis. Environ. Toxicol. Chem. 20, 2383–2396. doi:10.1002/etc.5620201034

Di Toro, D.M., Mahony, J.D., Kirchgraber, P.R., O'Byrne, A.L., Pasquale, L.R., Piccirilli, D.C., 1986. Effects of nonreversibility, particle concentration, and ionic strength on heavy-metal sorption. Environ. Sci. Technol. 20, 55–61. doi:10.1021/es00143a006

Drever, J.I., 1997. The geochemistry of natural waters: surface and groundwater environments - 3rd ed. Prentice Hall, Upper Saddle River, N.J.

Dwane, G.C., Tipping, E., 1998. Testing a humic speciation model by titration of copper-amended natural waters. Environ. Int. 24, 609–616. doi:10.1016/S0160-4120(98)00046-4

El Ganaoui, O., Schaaff, E., Boyer, P., Amielh, M., Anselmet, F., Grenz, C., 2004. The deposition and erosion of cohesive sediments determined by a multi-class model. Estuar. Coast. Shelf Sci. 60, 457–475. doi:10.1016/j.ecss.2004.02.006

Etchanchu, D., 1988. Géochimie des eaux du bassin de la Garonne : transferts de matières dissoutes et particulaires vers l'Océan Atlantique (PhD thesis). Université Paul Sabatier, Toulouse, France, 178 p.

Etchanchu, D., Probst, J.L., 1988. Evolution of the chemical composition of the Garonne River water during the period 1971–1984. Hydrol. Sci. J. 33, 243–256. doi:10.1080/02626668809491246

Farley, K.J., Carbonaro, R.F., Fanelli, C.J., Costanzo, R., Rader, K.J., Di Toro, D.M., 2011. TICKET-UWM: A coupled kinetic, equilibrium, and transport screening model for metals in lakes. Environ. Toxicol. Chem. 30, 1278–1287. doi:10.1002/etc.518

Farley, K.J., Rader, K.J., Miller, B.E., 2008. Tableau Input Coupled Kinetic Equilibrium Transport (TICKET) Model. Environ. Sci. Technol. 42, 838–844. doi:10.1021/es0625071

Gandois, L., Tipping, E., Dumat, C., Probst, A., 2010. Canopy influence on trace metal atmospheric inputs on forest ecosystems: Speciation in throughfall. Atmos. Environ. 44, 824–833. doi:10.1016/j.atmosenv.2009.11.028

Garay, S., Sauvage, S., Vervier, P., 2001. Hydromorphological control of phosphorus in a large free-flowing gravel bed river: The Garonne River (France). Regul. RIVERS-Res. Manag. 17, 461–472.

Garneau, C., 2014. Modélisation du transfert des éléments trace métalliques dans les eaux de surface. Université Paul Sabatier - Toulouse III, Toulouse, France.

Garneau, C., Sauvage, S., Probst, A., Sánchez-Pérez, J.M., 2015. Modelling of trace metal transfer in a large river under different hydrological conditions (the Garonne River in southwest France). Ecol. Model., Special Issue: Ecological Modelling for Ecosystem Sustainability: Selected papers presented at the 19th ISEM Conference, 28-31 October 2013, Toulouse, France 306, 195–204. doi:10.1016/j.ecolmodel.2014.09.011

Graba, M., Kettab, A., Sauvage, S., Sánchez Pérez, J.M., 2012. On modeling chronic detachment of periphyton in artificial rough, open channel flow. Desalination Water Treat. 41, 79–87. doi:10.1080/19443994.2012.664681

Guéguen, C., Dominik, J., 2003. Partitioning of trace metals between particulate, colloidal and truly dissolved fractions in a polluted river: the Upper Vistula River (Poland). Appl. Geochem. 18, 457–470. doi:10.1016/S0883-2927(02)00090-2

Hatten, J.A., Goñi, M.A., Wheatcroft, R.A., 2012. Chemical characteristics of particulate organic matter from a small, mountainous river system in the Oregon Coast Range, USA. Biogeochemistry 107, 43–66. doi:10.1007/s10533-010-9529-z

Hedges, J.I., Clark, W.A., Quay, P.D., Richey, J.E., Devol, A.H., Santos, U. de M., 1986. Compositions and fluxes of particulate organic material in the Amazon River. Limnol. Oceanogr. 31, 717–738.

Hindmarsh, A.C., Brown, P.N., Grant, K.E., Lee, S.L., Serban, R., Shumaker, D.E., Woodward, C.S., 2005. SUNDIALS: Suite of Nonlinear and Differential/Algebraic Equation Solvers. ACM Trans Math Softw 31, 363–396. doi:10.1145/1089014.1089020

Honeyman, B.D., Santschi, P.H., 1988. Metals in aquatic systems. Environ. Sci. Technol. 22, 862–871. doi:10.1021/es00173a002

Ji, Z.-G., Hamrick, J.H., Pagenkopf, J., 2002. Sediment and metals modeling in shallow river. J. Environ. Eng. 128, 105–119. doi:10.1061/(ASCE)0733-9372(2002)128:2(105)

Johansson, H., Lindström, M., Håkanson, L., 2001. On the modelling of the particulate and dissolved fractions of substances in aquatic ecosystems — sedimentological and ecological interactions. Ecol. Model. 137, 225–240. doi:10.1016/S0304-3800(00)00439-7

Kimball, B.A., Runkel, R.L., 2009. Spatially Detailed Quantification of Metal Loading for Decision Making: Metal Mass Loading to American Fork and Mary Ellen Gulch, Utah. Mine Water Environ. 28, 274–290. doi:10.1007/s10230-009-0085-5

Leleyter, L., Probst, J.-L., 1999. A new sequential extraction procedure for the speciation of particulate trace elements in river sediments. Int. J. Environ. Anal. Chem. 73, 109–128. doi:10.1080/03067319908032656

Lindenschmidt, K., Wodrich, R., Hesse, C., 2006. The effects of scaling and model complexity in simulating the transport of inorganic micropollutants in a lowland river reach. Water Qual. Res. J. Can. 41, 24–36.

Lofts, S., Tipping, E., 1998. An assemblage model for cation binding by natural particulate matter. Geochim. Cosmochim. Acta 62, 2609–2625.

Lofts, S., Tipping, E., 2000. Solid-solution metal partitioning in the Humber rivers: application of WHAM and SCAMP. Sci. Total Environ. 251–252, 381–399. doi:10.1016/S0048-9697(00)00418-6

Ludwig, J.A., Wilcox, B.P., Breshears, D.D., Tongway, D.J., Imeson, A.C., 2005. Vegetation Patches and Runoff-Erosion as Interacting Ecohydrological Processes in Semiarid Landscapes. Ecology 86, 288–297. doi:10.1890/03-0569

Ludwig, W., Probst, J.-L., Kempe, S., 1996. Predicting the oceanic input of organic carbon by continental erosion. Glob. Biogeochem. Cycles 10, 23–41.

Meybeck, M., 1982. Carbon, nitrogen, and phosphorus transport by world rivers. Am J Sci 282, 401–450.

Neal, C., Robson, A.J., Jeffery, H.A., Harrow, M.L., Neal, M., Smith, C.J., Jarvie, H.P., 1997. U.K. Fluxes to the North Sea, Land Ocean Interaction Study (LOIS) Rivers Basins Research, the First Two YearsTrace element inter-relationships for the Humber rivers: inferences for hydrological and chemical controls. Sci. Total Environ. 194, 321–343. doi:10.1016/S0048-9697(96)05373-9

Neitsch, S.L., Arnold, J.G., Kiniry, J.R., Williams, J.R., 2009. Soil and Water Assessment Tool - Theoretical Documentation. Texas A&M University, USA, Agricultural Research Service and Blackland Research Centre, Texas, USA.

Nimick, D.A., Gammons, C.H., Cleasby, T.E., Madison, J.P., Skaar, D., Brick, C.M., 2003. Diel cycles in dissolved metal concentrations in streams: Occurrence and possible causes. Water Resour. Res. 39, 1247. doi:10.1029/2002WR001571

Nimick, D.A., Gammons, C.H., Parker, S.R., 2011. Diel biogeochemical processes and their effect on the aqueous chemistry of streams: A review. Chem. Geol. 283, 3–17. doi:10.1016/j.chemgeo.2010.08.017

Oeurng, C., Sauvage, S., Sánchez-Pérez, J.-M., 2010. Dynamics of suspended sediment transport and yield in a large agricultural catchment, southwest France. Earth Surf. Process. Landf. 35, 1289–1301. doi:10.1002/esp.1971

Oliver, M.A., 1997. Soil and human health: a review. Eur. J. Soil Sci. 48, 573–592. doi:10.1111/j.1365-2389.1997.tb00558.x

Pardé, M., 1935. Le régime de la Garonne. Rev. Géographie Pyrén. Sud-Ouest 6, 105–262.

Parkhurst, D.L., Appelo, C.A.J., 1999. User's guide to PHREEQC (Version 2) - A Computer Program for Speciation, Batch-Reaction, One-Dimensional Transport, and Inverse Geochemical Calculations (No. Water-Resources Investigations Report 99-4259). Denver, Co.

Partheniades, E., 1965. Erosion and deposition of cohesive soils. J. Hydraul. Eng. Div. ACSE 91 105–139.

Periáñez, R., 2004. The dispersion of 137Cs and 239,240Pu in the Rhone River plume: a numerical model. J. Environ. Radioact. 77, 301–324. doi:10.1016/j.jenvrad.2004.03.013

Peyrard, D., Sauvage, S., Vervier, P., Sánchez Pérez, J.M., Quintard, M., 2008. A coupled vertically integrated model to describe lateral exchanges between surface and subsurface in large alluvial floodplains with a fully penetrating river. Hydrol. Process. 22, 4257–4273. doi:10.1002/hyp.7035

Probst, A., Hernandez, L., Probst, J.L., 2003. Heavy metals partioning in three French forest soils by sequential extraction procedure. J. Phys. IV Proc. 107, 1103–1106. doi:10.1051/jp4:20030493

Probst, J.-L., 1983. Hydrologie de la Garonne, modèle de mélanges, bilan de l'érosion, exportation des phosphates et des nitrates (PhD thesis). Université Paul Sabatier, Toulouse, France, 148 p.

Probst, J.-L., 1992. Géochimie et hydrologie de l'érosion continentale. Mécanismes, bilan global actuel et fluctuations au cours des 500 derniers millions d'années. Sci. Géologiques Mem., ed. Univ. Strasbourg, 94, Strasbourg, France, 167 p.

Probst, J.-L., Bazerbachi, A., 1986. Transport en solution et en suspension par la Garonne supérieure. Sci. Géologiques Bull. 39, 79–98.

Roussiez, V., Probst, A., Probst, J.-L., 2013. Significance of floods in metal dynamics and export in a small agricultural catchment. J. Hydrol. 499, 71–81. doi:10.1016/j.jhydrol.2013.06.013

Runkel, R.L., Bencala, K.E., Kimball, B.A., 1999. Modeling solute transport and geochemistry in streams and rivers using OTIS and OTEQ. Presented at the U.S. Geological Survey Toxic Substances Hydrology Program: Proceedings of The Technical Meeting, D. W. Morganwalp and H. T. Buxton, Charleston SC, pp. 120–127.

Saltelli, A., Annoni, P., 2010. How to avoid a perfunctory sensitivity analysis. Environ. Model. Softw. 25, 1508–1517. doi:10.1016/j.envsoft.2010.04.012

Sánchez-Pérez, J.-M., Probst, A., Gerino, M., Sauvage, S., Aubert, D., Devault, D., Tackx, M., Boulêtreau, S., Dalger, D., Delmas, F., Dubernet, J.F., Durbe, G., Henry, M., Julien, F., Lim, P., Merlina, G., Mamoudou, M., Pinelli, E., Probst, J.-L., Vervier, P., 2006. Fluvial transport and transformation of heavy metals, pesticides and biogenic elements in the Garonne river continuum system. Presented at the Man and River System II, Interactions among Rivers, their Watershed and the Sociosystem, Paris, France, pp. 49–51.

Santore, R.C., Driscoll, C.T., 1995. The CHESS model for calculating chemical equilibria in soils and solutions, in: SSSA Special Publication.

Sauvage, S., Teissier, S., Vervier, P., Améziane, T., Garabétian, F., Delmas, F., Caussade, B., 2003. A numerical tool to integrate biophysical diversity of a large regulated river: hydrobiogeochemical bases. The case of the Garonne River (France). River Res. Appl. 19, 181–198. doi:10.1002/rra.698

Semhi, K., 1996. Erosion et transferts de matières sur le bassin versant de la Garonne. Influence de la sécheresse (PhD thesis). Université Louis Pasteur, Strasbourg, France, 203 p.

Semhi, K., Amiotte Suchet, P., Clauer, N., Probst, J.-L., 2000a. Impact of nitrogen fertilizers on the natural weathering-erosion processes and fluvial transport in the Garonne basin. Appl. Geochem. 15, 865–878. doi:10.1016/S0883-2927(99)00076-1

Semhi, K., Clauer, N., Probst, J.L., 2000b. Strontium isotope compositions of river waters as records of lithology-dependent mass transfers: the Garonne river and its tributaries (SW France). Chem. Geol. 168, 173–193. doi:10.1016/S0009-2541(00)00226-6

Shi, Z., Allen, H.E., Di Toro, D.M., Lee, S.-Z., Flores Meza, D.M., Lofts, S., 2007. Predicting cadmium adsorption on soils using WHAM VI. Chemosphere 69, 605–612. doi:10.1016/j.chemosphere.2007.03.001

Siegel, D.I., 1983. Isotope Studies of Hydrologic Processes. Eos Trans. Am. Geophys. Union 64, 430. doi:10.1029/EO064i026p00430

S.M.E.P.A.G., 1989. Atlas hydraulique de la Garonne: du Pont du Roy au Bec d'Ambès, (Schéma de protection contre les eaux de la Garonne ; 2). Syndicat mixte d'étude et de programmation pour l'aménagement de la Garonne, Toulouse, France.

Steiger, J., Corenblit, D., Vervier, P., Tesseyre, D., 2001a. Etude de la dynamique fluviale de la Garonne Toulousaine. Centre d'écologie des systèmes aquatiques continentaux - CESAC, Toulouse, France.

Steiger, J., Gurnell, A.M., 2003. Spatial hydrogeomorphological influences on sediment and nutrient deposition in riparian zones: observations from the Garonne River, France. Geomorphology 49, 1–23. doi:10.1016/S0169-555X(02)00144-7

Steiger, J., Gurnell, A.M., Ergenzinger, P., Snelder, D., 2001b. Sedimentation in the riparian zone of an incising river. Earth Surf. Process. Landf. 26, 91–108. doi:10.1002/1096-9837(200101)26:1<91::AID-ESP164>3.0.CO;2-U

Stigter, T.Y., van Ooijen, S.P.J., Post, V.E.A., Appelo, C.A.J., Carvalho Dill, A.M.M., 1998. A hydrogeological and hydrochemical explanation of the groundwater composition under irrigated land in a Mediterranean environment, Algarve, Portugal. J. Hydrol. 208, 262–279. doi:10.1016/S0022-1694(98)00168-1

Teissier, S., Sauvage, S., Vervier, P., Garabétian, F., Sánchez-Pérez, J.-M., 2008. A mass-balance approach to estimate in-stream processes in a large river. Hydrol. Process. 22, 420–428. doi:10.1002/hyp.6614

Tercier-Waeber, M.-L., Hezard, T., Masson, M., Schäfer, J., 2009. In Situ Monitoring of the Diurnal Cycling of Dynamic Metal Species in a Stream under Contrasting Photobenthic Biofilm Activity and Hydrological Conditions. Environ. Sci. Technol. 43, 7237–7244. doi:10.1021/es900247y

Tessier, A., Campbell, P.G.C., Bisson, M., 1979. Sequential extraction procedure for the speciation of particulate trace metals. Anal. Chem. 51, 844–851. doi:10.1021/ac50043a017

Thorstenson, D.C., Parkhurst, D.L., 2002. Calculation of individual isotope equilibrium constants for implementation in geochemical models (No. 02–4172), U.S. Geological Survey, Water-Ressources Investigations. Denver Colorado.

Tipping, E., 1994. WHAMC—A chemical equilibrium model and computer code for waters, sediments, and soils incorporating a discrete site/electrostatic model of ion-binding by humic substances. Comput. Geosci. 20, 973–1023. doi:10.1016/0098-3004(94)90038-8

Tipping, E., Lofts, S., Lawlor, A.J., 1998. Modelling the chemical speciation of trace metals in the surface waters of the Humber system. Sci. Total Environ. 210–211, 63–77.

Tipping, E., Lofts, S., Sonke, J.E., 2011a. Humic Ion-Binding Model VII: a revised parameterisation of cation-binding by humic substances. Environ. Chem. 8, 225. doi:10.1071/EN11016

Tipping, E., Lofts, S., Sonke, J.E., 2011b. Humic ion-binding model VII: a revised parameterisation of cation-binding by humic substances. Environ. Chem. 8, 225–235.

Tipping, E., Rieuwerts, J., Pan, G., Ashmore, M.R., Lofts, S., Hill, M.T.R., Farago, M.E., Thornton, I., 2003. The solid–solution partitioning of heavy metals (Cu, Zn, Cd, Pb) in upland soils of England and Wales. Environ. Pollut. 125, 213–225. doi:10.1016/S0269-7491(03)00058-7

Trancoso, A.R., Braunschweig, F., Chambel Leitão, P., Obermann, M., Neves, R., 2009. An advanced modelling tool for simulating complex river systems. Sci. Total Environ. 407, 3004–3016. doi:doi: 10.1016/j.scitotenv.2009.01.015

Uehlinger, U., Bührer, H., Reichert, P., 1996. Periphyton dynamics in a floodprone prealpine river: evaluation of significant processes by modelling. Freshw. Biol. 36, 249–263. doi:10.1046/j.1365-2427.1996.00082.x

van Breukelen, B.M., Röling, W.F.M., Groen, J., Griffioen, J., van Verseveld, H.W., 2003. Biogeochemistry and isotope geochemistry of a landfill leachate plume. J. Contam. Hydrol. 65, 245–268. doi:10.1016/S0169-7722(03)00003-2

van Griensven, A., Meixner, T., Grunwald, S., Bishop, T., Diluzio, M., Srinivasan, R., 2006. A global sensitivity analysis tool for the parameters of multi-variable catchment models. J. Hydrol. 324, 10–23. doi:10.1016/j.jhydrol.2005.09.008

Veyssy, E., Colas, C., Etcheber, H., Maneux, E., Probst, J.-L., 1996. Transports fluviaux de carbone organique par la Garonne à l'entrée de l'estuaire de la Gironde. Sci. Géologiques Bull. 49, 127–153.

Weng, L., Temminghoff, E.J.M., Lofts, S., Tipping, E., Van Riemsdijk, W.H., 2002. Complexation with dissolved organic matter and solubility control of heavy metals in a sandy soil. Environ. Sci. Technol. 36, 4804–4810. doi:10.1021/es0200084

Wright, J.C., Mills, I.K., 1967. Productivity studies on the Madison River, Yellowstone National Park. Limnol. Oceanogr. 12, 568–577. doi:10.4319/lo.1967.12.4.0568

Ziervogel, K., Bohling, B., 2003. Sedimentological parameters and erosion behaviour of submarine coastal sediments in the south-western Baltic Sea. Geo-Mar. Lett. 23, 43–52. doi:10.1007/s00367-003-0123-4

8 Supplementary material

8.1 The WHAM implementation

This section reviews the main properties of WHAM and the numerical solutions proposed to solve it.

The WHAM model includes three sub-models to simulate three SPM constituents:

- The Humic Ion-Binding Model VII (M7) for humic acids and fulvic acids
- A surface complexation model (SCM) for iron, manganese, aluminium oxides
- A cation exchange model for clay minerals

Two processes allow cations to be retained by the SPM. The first one is through binding of cations to discrete binding sites over the organic matter (humic and fulvic acids) and metal oxides. The second process considers that at equilibrium, the phase can still be charged. A diffuse layer is then computed in which counterions accumulate based on Donnan equilibrium. This diffuse layer is present around all three types of phases (organic matter, metal oxides and clay minerals).

The WHAM was represented as a set of implicit algebraic equations (equation 17).

$$0 = F(x, y, \theta) \qquad 17$$

Where:

- F are the state equations
- x are the state variables of the model
- y are the input variables
- θ are the parameters.

The state variables were:

- For the whole solution
    - The free ionic concentration of each ion in solution
    - The ionic strength
    - The total volume of the diffuse layer

- For M7 and the SCM
    - The free binding sites concentration
    - The surface charge of the phase
- For the M7, the SCM and the clay model
    - The ratio of counterions in the diffuse layer versus ions in the true solution

The state functions are closely related to the state variables and were chosen such as their value at equilibrium is null:

- For the whole solution
    - The mass balance of each ion in solution
    - The difference between the estimated and the calculated ionic strength
    - The difference between the estimated and the calculated volume of the diffuse layer
- For M7 and the SCM
    - The mass balance of each binding site
    - The difference between the estimated and the calculated global charge of the phase
- For M7, the SCM and the clay model
    - The residual charge in the diffuse layer

The mass balance was defined as the difference between the input total concentration and the sum of each complex of the ion or binding site. Therefore, at equilibrium, the mass balance is zero.

In short, WHAM required 3 global state variables, 52 state variables per M7 instance, 5 state variables per SCM instance, 1 state variable per clay model instance and n state variables for the n chemical species for which mass-balance was required. Therefore, a model of trace metal which includes eight major ions, two M7 instances for humic and fulvic acids sorption, two SCM instances for adsorption on iron and manganese oxides and one clay model instance, requires the simultaneous solution of 122 state equations.

The input variables were:

- The total concentration of the ions
- The chemical state of the solution (pH, temperature, pCO2)
- The concentration of each phase of the three submodels (M7, SCM and the clay model)

Finally, the submodels of WHAM require a large number of parameters

- M7: 10 parameters plus 2 per ion in solution
- SCM: 12 parameter plus one per ion in solution
- Clay model: 1 parameter for cationic exchange capacity (CEC)

However, default parameterizations were proposed by Tipping et al. (2011a) for M7, and Lofts and Tipping (1998) for the SCM, based on calibration and validation over a large number of datasets. The only

exception was the CEC, which depended on the clay characteristics. In the scope of these works, we chose to use the default parameters proposed by Tipping et al. (2011a) and Lofts and Tipping (1998), as they were calibrated over >300 datasets.

8.2 Numerical solution

The numerical solution of WHAM must be robust under a wide variation in the inputs. The robustness of the solution was ensured by the implementation of two solving techniques. The first one relayed on the numerical library KINSOL from the SUNDIALS library (Hindmarsh et al., 2005) which implements approximated Newton-Raphson solving strategies adapted to large systems of equations. However, as the Newton-Raphson method is known to be prone to failure when the initial estimate of the solution is far from the true solution, a second slower method was implemented to insure convergence even when the initial estimates were far from the solution. This second method is based on continued fractions (Tipping, 1994). It considers every state variable independently and proposes a new estimate of the solution based on the nature of the state variable. The free ions and binding sites concentrations were updated based on equation 18.

$$x_{estimate_{i+1}} = x_{estimate_i} \times \frac{X_{obs}}{X_{calc}} \quad 18$$

Where:

- $x_{estimate_i}$ is the actual estimate of the free ion concentration
- $x_{estimate_{i+1}}$ is the next estimate of the free ion concentration
- X_{obs} is the total ion concentration observed
- X_{calc} is the total ion concentration calculated by WHAM

In the scope of chemical equilibrium problem, equation 18 will converge asymptotically to the solution almost independently of the initial estimate. However, the convergence being asymptotic, a large number of iterations could be necessary. Nevertheless, the continued fraction algorithm proved to be efficient on chemical models (Tipping, 1994).

A strategy based on both the Newton-Raphson approach and this alternative solution proved to be a very robust numerical scheme, capable of converging slowly when the initial estimate was far from the solution, then quickly when the solution has been cornered. In practice, in the scope of river modelling, the slowly converging scheme was necessary for the first time that the model was solved and for important perturbations of the water quality. Then, the model was easily updated on the basis of the previous solution with the KINSOL algorithm.